Bureau of Mineral Resources, Geology & Geophysics

R E C O R D

Record No. 1989/8

BUREAU OF MINERAL RESOURCES LIBRARY 18 APR 1989 CANBERRA, A.C.T.

CALIBRATION OF THE BMR AIRBORNE GAMMA-RAY SPECTROMETERS UPWARD-LOOKING DETECTOR, FEBRUARY 1989.

BMR PUBLICATIONS COMPACTUS (LENDING SECTION)

C.4

by

B.R.S. Minty and L.M. Richardson

The information contained in this report has been obtained by the Bureau of Mineral Resources, Geology and Geophysics as part of the policy of the Australian Government to assist in the exploration and development of mineral resources. It may not be published in any form or used in a company prospectus or statement without the permission in writing of the Director.

DEPARTMENT OF PRIMARY INDUSTRIES & ENERGY

BUREAU OF MINERAL RESOURCES, GEOLOGY AND GEOPHYSICS

Record No. 1989/8

CALIBRATION OF THE BMR AIRBORNE GAMMA-RAY SPECTROMETERS UPWARD-LOOKING DETECTOR, FEBRUARY 1989.

by

B.R.S. Minty and L.M. Richardson
(Division of Geophysics)

CONTENTS

FIGURES Page

TABLES

ABSTRACT

The correct estimation and removal of 'background' gamma-radiation flux is crucial to the processing of airborne radiometric data because its incorrect removal introduces gross levelling errors into the data. This record describes the calibration of the BMR's airborne gamma-ray spectrometer for the detection of background radiation according to the method of GeoMetrics (1979) and the method of the Geological Survey of Canada (Grasty et al., 1988). Calibration flights were flown both offshore and onshore near Mount Gambier (SE South Australia) and over Lake Hume (New South Wales). These data have enabled us to calculate firstly, aircraft background, and secondly, sensitivity coefficients that enable the calculation of cosmic and atmospheric (radon) background using the systems 3-6 MeV cosmic window and upward-looking detector.

1. INTRODUCTION

In airborne gamma-ray spectrometry ('radiometrics') any radiation not originating from the ground is of no geological interest and must be removed as 'background' during processing. The three main sources of background radiation are atmospheric ^{222}Rn and its daughter products, cosmic radiation, and radioactivity from the aircraft and its contents. The correct estimation and removal of the background radiation flux is crucial to the processing of airborne radiometric data because its incorrect removal introduces gross errors into the data between adjacent flight lines.

The contribution of background radiation to the observed spectrum are currently estimated in a number of ways:

(a) by recording the radiation level at a terrain clearance of 1000 metres before and after each flight;
(b) by recording the radiation level while flying over a large body of water at the survey terrain clearance;
(c) by the use of an "upward-looking" detector to monitor the background radiation level continuously.

Minty (1988) reviewed airborne radiometric processing techniques and discussed the relative merits of the above background estimation techniques. A continuous estimation of background, such as (c) above, is obviously preferable to interpolation between estimates obtained many hours apart.

The BMR airborne gamma-ray spectrometer system used for reconnaisance surveying includes a 4.2 litre "upward-looking" crystal mounted immediately above the 16.8 litre "downward-looking" crystal pack. The upward-looking crystal is thus partially shielded by the downward-looking crystal against radiation from below, and it is this 'directional sensitivity' which gives the system the ability to discriminate between radiation from the atmosphere and from the ground. The detectors record data from four adjustable windows in the gamma-ray spectrum. These are usually set as: total count (TC) window (0.4-3.0 MeV), potassium (K) window (1.35-1.57 MeV), uranium (U) window (1.63-1.89 MeV), and the thorium (Th) window

(2.42-2.82 MeV). In addition, spectra for the downward-looking detector, measured by 256 channels between 0.0 and 3.0 MeV, are summed over 300 second intervals, and for each line, and these are also recorded.

Prior to the 1988 field season, a 'cosmic' window (3.0-6.0 MeV) was added to the downward-looking detector. This cosmic window enabled the spectrometer system to be rigourously calibrated for the continuous estimation of cosmic background radiation for the first time. The calibration data were acquired during March 1988 on calibration flights both offshore and onshore near Mount Gambier in South Australia, and over Lake Hume in New South Wales.

There are currently two published techniques for computing radiometric backgrounds using upward-looking detectors. The method of GeoMetrics (1979) uses 4 upward-looking windows (TC, K, U, Th) and a 3.0-6.0 MeV 'cosmic' window in the downward-looking detector. More recently, the Geological Survey of Canada (Grasty & others, 1988) have published a technique that requires only a single upward-looking uranium window and no cosmic window. The purpose of this record is to document the results of calibrating the spectrometer according to both techniques. Section 2 describes the calibration using the GeoMetrics technique and section 3 the calibration using the method of the Geological Survey of Canada (GSC).

2. METHOD OF GEOMETRICS

2.1 Calibration technique

The calibration technique used in the method of GeoMetrics (1979) can be broadly divided into two phases:

(a) The determination of aircraft and cosmic background for each of the detectors. We require the aircraft spectrum (shape and amplitude), and the cosmic spectrum normalised to the cosmic window countrate.

(b) The coefficients l and m, which describe the relative sensitivity of the upward-looking detector to the downward-looking detector for radiation from the ground and atmosphere respectively.

Aircraft and cosmic background

This procedure makes use of the fact that in the lower atmosphere the cosmic spectrum has a near constant shape, but its amplitude decreases with decreasing altitude (Aviv, R. and Vulcan, V., 1983). Also, at energies greater than 3.0 MeV all radiation is cosmic in origin. Irrespective, therefore, of other sources of radiation, the cosmic contribution in any window is proportional to the total count between say, 3.0 and 6.0 MeV; i.e., if we know the shape of the cosmic spectrum for a particular installation, then for each detector we can use the 3.0-6.0 MeV countrate to calculate the cosmic contribution in any particular window.

The strategy is to collect full spectra over water at a number of different heights (say 1, 2, ... 5 km) where there is no airborne ^{214}Bi, e.g. offshore where the prevailing winds are landwards, or alternatively after a high-pressure front arrives, or after general precipitation in the calibration area, since all these tend to reduce atmospheric radioactivity to low levels (Fritzsche, 1982). The measured spectra are each the sum of the aircraft component (constant) and the cosmic component, and these components can be resolved in two ways:

(a) Because the aircraft component is constant, the cosmic component can be calculated by taking the **difference between any two spectra**, then normalising this spectrum to the 3.0-6.0 MeV countrate. This procedure can be repeated for each combination of heights and the results averaged. The aircraft spectrum is obtained by subtracting the cosmic background spectrum from any of the observed spectra. Again, the results can be averaged.

(b) Alternatively, a **graphical technique**, used by local contractors, can be employed (M. Morse - personal communication). A linear regression of the cosmic window countrate on any other particular window yields that windows cosmic sensitivity (slope of regression line) and aircraft background (zero intercept). We

favoured this approach for our calibration as deviations from the linear relationship give a clear indication of the presence of radon.

Atmospheric radon background

Consider the following crystal configuration:

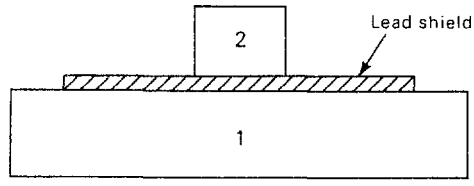

Let 1 and 2 designate the downward-looking and upward-looking crystals respectively. The down crystal 'sees' a radiation rate (I_1) composed of the ground signal (I_g) and the air signal (I_a), plus aircraft (A_1) and cosmic (C_1) background, i.e.

$$I_1 = I_g + I_a + A_1 + C_1$$

Similarly, $$I_2 = lI_g + mI_a + A_2 + C_2$$

where l and m are the relative sensitivities of the upward-looking detector to the downward-looking detector for radiation from the ground and atmosphere respectively.

For calibration data acquired by flying at different heights from water to land, and after correcting the 'over-land' leg of each line for all background by subtracting the 'over-water' leg averages, we have

$$A_1 = A_2 = C_1 = C_2 = I_a = 0$$

Therefore, $$I_1 = I_g$$

$$I_2 = lI_g$$

and $$l = I_2/I_1$$

Note that, owing to 'skyshine' (backscattering of photons by the air), l should decrease with height for broad sources, i.e., $l = f(h)$. This height dependence should not be severe for windows above 1.0 MeV, since the average energy of backscattered radiation is substantially less than 1.0 MeV.

The factor m is calculated from 'over-water' data at survey height when radon + daughters are present. This can be done a number of times for various radon concentrations and the results averaged.

In this case, $I_g = 0$ and A_1, A_2, C_1, and C_2 can be measured and removed as described earlier.

Therefore, $I_1 = I_a$

$I_2 = mI_a$

and $m = I_2/I_1$

Note that m changes with height, since as height decreases, the earth intercepts an increasing fraction of the volume of radioisotope-bearing air and this is more severe for the down detector than the up detector. m is also uncertain in its determination because of the unknown shape of the vertical radon concentration profile. This uncertainty can be minimised by ensuring that all calibration and survey flights are flown after air turbulence has mixed the radon vertically in the atmosphere.

Atmospheric background can thus be estimated as follows: both the up and down counting rates are corrected for aircraft and cosmic background, to give

$$I_1 = I_g + I_a$$

$$I_2 = lI_g + mI_a$$

or $$I_a = (I_2 - lI_1)/(m-l) \qquad \text{.....(1)}$$

which is subtracted from the down-window countrates to give background corrected data.

2.2 Data acquisition

The radon-free, high altitude flights used for cosmic and aircraft background determination were flown 10 km offshore from Mount Gambier (SE South Australia). The prevailing winds are from the west-southwest over the Southern Ocean and the area was specifically chosen for its low atmospheric radon content. The topography in the Mount Gambier area is subdued. Consequently we also used this area to acquire the offshore-onshore calibration data required to calculate the sensitivity constants, 1. The only assumption made here is that if radon is present, then its concentration and distribution was the same over both the land and water - i.e. we can use the over-water data to subtract all background. Calibration data for the coefficients, m, were obtained over Lake Hume.

The data were acquired as follows:

(a) **Cosmic and aircraft spectra:** Full spectra 10 km offshore from Mount Gambier were collected at each of 1, 2, ... 5 km altitude. Ten minutes of data acquisition at each altitude was considered sufficient. A further 10 minutes offshore at 150m altitude was flown to serve as a further check on the aircraft background.

(b) **The coefficient 1:** 3 lines were flown at each of the following altitudes: 100m, 150m, 200m, 250m, 300m, and 350m. This range of altitudes reflects those found in regional airborne surveys undertaken by BMR. Each line was of 10 minutes duration - i.e. 5 minutes over water and 5 minutes over land.

(c) **The coefficient m:** These data were acquired over Lake Hume. One 15 minute line at each of the following altitudes were flown: 100m, 150m, 200m, 250m, 300m, and 350m.

The calibration data were acquired during the period 24-26 March 1988 and on the 29 March 1988. The crew consisted of Mr. J. Floate (pilot), Mr. D. Pownall (electronics technician), and Mr. L.M. Richardson (geophysicist/party leader). Two full sets of calibration

data were acquired. The first set used the standard BMR regional survey detector configuration of 16.8 litres downward-looking crystals and 4.2 litres of upward-looking crystals mounted in the rear luggage compartment. The second set of data was acquired using a total of 33.6 litres of downward-looking crystals and 8.4 litres of upward-looking crystals. This was achieved by adding a second 16.8/4.2 litre pack forward of the luggage compartment. The 33.6/8.4 litre detector configuration is used on high sensitivity surveys.

2.3 Discussion of results

Initially, we used the differences between high altitude spectra (see page 3) to obtain cosmic and aircraft spectrum estimates. However, there appears to be a systematic bias in the cosmic spectrum estimates using this method. Specifically, the cosmic spectrum results obtained by normalising the difference of the spectra measured at 5000 metres and 4000 metres (denoted by '5000-4000', say) are greater than '5000-3000', which in turn are greater than '5000-2000' and so on. Similarly, '4000-3000' yields estimates greater than '4000-2000' etc.. Whilst this bias is not large or all-pervasive, the trend is evident. We suspect that this was due to the calibration environment not being entirely radon-free, with the radon concentration decreasing with increasing altitude. An analysis of the multichannel 'whole-line' spectra (discussed later) confirms this was the case.

Figures 1-8 show the regression plots used to determine the cosmic and aircraft background estimates using the graphical method. We interpret the higher countrates at 1000 metres and 2000 metres (single detector, Figs 1-4) and 1000 metres (twin detectors, Figs 5-8) as being the result of the presence of radon at these altitudes. These data were therefore not used in the regression. The normalised cosmic background and the aircraft background for each window are given in Tables 1 and 2. The cosmic countrate in any particular window can be calculated by multiplying the observed cosmic countrate with the appropriate factor listed.

The upward-looking detectors do not have the 3.0-6.0 MeV cosmic window and the next step in the calibration is to find some way of relating the observed 'cosmic+aircraft' countrate in the downward-looking detectors to that in the upward-looking detectors. We have achieved this by applying a linear regression (y=bx) to the observed upward and downward-looking countrates on the offshore legs of the 'offshore-onshore' Mount Gambier calibration data. These data should be near radon-free, and the offshore countrates should thus be due only to cosmic and aircraft radiation. The regression coefficients are listed in Table 3. These define the relative sensitivity of the upward to the downward-looking detectors for cosmic and aircraft radiation.

The l-sensitivity constants which relate the sensitivity of the upward to the downward-looking detectors for radiation from the ground were calculated using the Mount Gambier offshore-onshore data. The results are plotted as a function of altitude in Figures 9-12 (single detector) and Figures 13-16 (twin detectors). Three lines at each altitude were flown. At most altitudes each line yielded an estimate for l within $\pm$10% of the mean for that altitude. This is consistent with previously published calibration results of this type (Fritzche, 1982). However, above 250m and specifically at 350m the spread of estimates is very poor. Also, the altitude dependance does not appear to be strong above 250 metres, and for these reasons the linear regression is only applied to altitudes up to and including 250 metres. The regression coefficients are listed in Table 4.

The m-sensitivity constants were calculated from the Lake Hume data. The results as a function of altitude are plotted in Figures 17-20 (single detector) and Figures 21-24 (twin detectors). Again, we have chosen to apply the linear regression to altitudes at or below 250 metres. The regression coefficients are given in Table 5.

The procedure for estimating and removing background radiation is thus as follows:

(a) Calculate the cosmic contribution to each window of the downward-looking detector using the cosmic window countrate and the factors listed in Table 1.

(b) Add the aircraft background (Table 2) to the cosmic background and subtract the total from the downward-looking detector window countrates.

(c) Calculate the cosmic+aircraft contribution to the upward-looking detectors window countrates using the sum obtained in (b) above and the regression coefficients in Table 3. Subtract this cosmic+aircraft contribution from the upward-looking detectors window countrates.

(d) Use equation (1) to calculate the radon contribution to the downward-looking detectors window countrates and subtract.

Figures 25-27 show multichannel spectra for aircraft, cosmic, and radon background for the twin detectors. These were calculated from the high altitude calibration data (cosmic and aircraft spectra) and the Lake Hume data (radon spectrum). Similar spectra for the single detector are noisier due to the poorer statistics, and we suggest that future high altitude calibration flights for multichannel calibration of this detector should be of 20 minutes duration each.

Having acquired the calibration data, we discovered that the whole-line multichannel spectra are corrupted to the extent that the accumulation time of the spectra extends 20 seconds beyond the end of each line. Nevertheless, the spectra have served as a useful check on the 4-channel calibration and are included for interest only. Figure 28 is an example of a cosmic spectrum estimate affected by airborne radon. This spectrum was obtained by subtracting the single detectors 2000 metre whole-line spectrum from the 4000 metre whole-line spectrum. The low at about 0.6 MeV is due to a higher concentration of radon at 2000 metres than at 4000 metres (c.f. 0.609 MeV ^{214}Bi peak in the radon spectrum).

Finally, Table 6 shows a typical 4-channel background spectrum (Lake Hume, single detector data) and its calculated component parts - i.e. cosmic, aircraft and atmospheric (radon) background. This gives an interesting insight into the relative contributions of each component to the observed background.

3. METHOD OF THE GEOLOGICAL SURVEY OF CANADA

Subsequent to acquiring the Mount Gambier/Lake Hume calibration data, the Geological Survey of Canada (GSC) published a new method of calculating radiometric backgrounds (Grasty & others, 1988). Part of the spectrometer calibration procedure for this technique (section 3.2) requires background corrected data exhibiting a range of uranium to thorium ratios. The Mount Gambier calibration data are not suitable in this respect. Consequently we have been unable to calibrate the twin detector system (33.6/8.4 litre configuration) for this technique. However, we have been able to use data from previous surveys to supplement the Mount Gambier/Lake Hume data in order to calibrate the single detector system for this method.

3.1 Theory (after Grasty & others, 1988)

The method is for calculating 'over-water' backgrounds in all windows using a single uranium upward-looking window. No cosmic window is required. Grasty (1979) found that the observed backgrounds in the total-count and potassium windows are linearly related to the uranium window background. Thus it is only necessary to monitor a single uranium upward-looking window to calculate the downward uranium window background. The total-count and potassium window background countrates can then be calculated from the uranium window background.

We assume the aircraft flies at a constant ground clearance and can therefore ignore any altitude dependance in the relative sensitivities of the upward to the downward-looking detectors for radiation from the ground and air. Also, we assume the cosmic contribution to each window's countrate is constant.

Let u = measured upward detector countrate (uranium window),

u_g = upward detector countrate originating in radiation from the ground,

u_b = 'over-water' background contribution to the upward detectors countrate,

and U = measured downward detector uranium window countrate,

U_g = downward detectors uranium window countrate originating in radiation from uranium in the ground,

U_b = 'over-water' background contribution to the downward detectors uranium window countrate,

and T = measured downward detector thorium window countrate,

T_g = downward detectors thorium window countrate originating from the ground,

T_b = 'over-water' background contribution to the downward detectors thorium window countrate. We assume this value to be constant.

Then we can relate the measured window countrates to their respective ground and background components as follows:

$$u = u_g + u_b \qquad \text{.....(2)}$$

$$U = U_g + U_b \qquad \text{.....(3)}$$

$$T = T_g + T_b \qquad \text{.....(4)}$$

Since u_g depends on the concentration of both uranium and thorium in the ground, and U_g and T_g also depend on the concentrations of uranium and thorium in the ground, we can relate u_g to U_g and T_g linearly as follows:

$$u_g = a_1 U_g + a_2 T_g \qquad \text{.....(5)}$$

where a_1 and a_2 are constants to be determined. Also, u_b will be linearly related to U_b and we can write

$$u_b = a_3 U_b + a_4 \qquad \text{.....(6)}$$

where a_3 and a_4 are constants to be determined.

If we substitute for u_b and u_g from equations (5) and (6) into equation (2) we get:

$$u = a_1U_g + a_2T_g + a_3U_b + a_4 \quad \text{.....(7)}$$

which from equations (3) and (4) gives

$$u = a_1U - a_1U_b + a_2T - a_2T_b + a_3U_b + a_4 \quad \text{.....(8)}$$

Equation (8) can then be rearranged to give U_b, the 'over-water' uranium background in terms of u, T, U and T_b as follows:

$$U_b = (u - a_1U - a_2(T - T_b) - a_4)/(a_3 - a_1) \quad \text{.....(9)}$$

3.2 Calibration

The calibration consists of determining the 5 constants in equation (9) - i.e. a_1, a_2, a_3, a_4, and T_b. In addition, we have to calculate the linear relationships between the uranium and total-count backgrounds, and between the uranium and potassium window backgrounds.

The constants a_3 and a_4 (equation (6)) can be calculated from over-water flights at the survey altitude. Obviously, the greater the range of values used for U_b and u_b, the greater the accuracy to which they will be determined. We used the offshore legs of the Mount Gambier offshore-onshore lines for low count u_b and U_b backgrounds, and the Lake Hume data for high count backgrounds. The results are given in Figure 29. The least-squares fit line shown in Figure 29 is defined by:

$$u_b = 0.281U_b + 0.106 \quad \text{.....(10)}$$

The constants a_1 and a_2 (equation (5)) require background corrected data for their calculation. Grasty & others (1988) propose two procedures:

(a) The use of data flown over both land and water. The over-water data are then used to subtract all background.

(b) The background over a particular section of line can be removed by subtracting the average countrate from an adjacent section of the line. The reason for this is that the difference between the average countrates must be due to differences in the ground concentration of the naturally occurring radioelements over the two sections of line.

The constants are determined by the least-squares solution of the following simultaneous equations (Grasty & others, 1988):

$$a_1\Sigma(U_g)^2 + a_2\Sigma U_g T_g = \Sigma u_g U_g \quad \ldots\ldots\ldots\ldots(11)$$

$$a_1\Sigma U_g T_g + a_2\Sigma(T_g)^2 = \Sigma u_g T_g \quad \ldots\ldots\ldots\ldots(12)$$

Grasty & others (1988) note that reliable estimates of a_1 and a_2 require a large range in the thorium to uranium ratios of the background corrected averages used. Also, if procedure (b) above is used, statistical errors are reduced if the line sections have a high average countrate section adjacent to a low countrate section for the background.

The Mount Gambier offshore-onshore lines did not have a sufficient range in thorium to uranium ratios for reliable estimates of a_1 and a_2 to be made. Consequently we supplemented these lines with offshore-onshore lines from the COEN 1:250000 sheet (project 520) and onshore lines from the TUREE CREEK and EDMUND 1:250000 sheet areas (project 509). In the case of project 509, procedure (b) above was used. The data used are summarised in Table 7. These data cover a range of thorium to uranium ratio values from 1.0 to 2.67.

The constants a_1 and a_2 were calculated from equations (11) and (12) to give:

$$u_g = 0.1162U_g + 0.01696T_g \quad \ldots\ldots\ldots(13)$$

Substituting for a_1, a_2, a_3, a_4 and a constant for T_b, we can use equation (9) to calculate the over-water uranium window countrate.

Finally, we establish the linear relationships between the uranium and total-count window backgrounds (Figure 30) and the uranium and potassium window backgrounds (Figure 31). In both cases we used the offshore legs of the Mount Gambier offshore-onshore lines for the low count backgrounds and the Lake Hume data for the high count backgrounds. The least-squares fit lines shown in Figures 30 and 31 are defined by

$$TC_b = 12.2U_b + 45.1 \quad \text{.....(14)}$$

and

$$K_b = 0.75U_b + 14.6 \quad \text{.....(15)}$$

The procedure for estimating the background radiation using this technique is then as follows:

(a) Establish the thorium background for the survey area. An over-water value would be ideal. Otherwise use the 1000 metre altitude background. This value is constant.

(b) Use equation (9), the values a_1=0.1162, a_2=0.01696, a_3=0.281, a_4=0.106, and the value for Tb from (a) above to evaluate the uranium window background for a particular time interval.

(c) Use equation (14) and (15) to calculate the total-count and potassium window backgrounds from the uranium window background.

4. DISCUSSION AND CONCLUSION

We have calibrated the BMR's airborne gamma-ray spectrometer for use with an upward-looking detector according to two published techniques.

The method of GeoMetrics (1979) is the more complex of the two. Ideally it requires two cosmic windows - one for each of the upward and downward-looking detectors. The BMR system has a single cosmic window in the downward-looking detector and we have used calibration data to linearly relate 'aircraft+cosmic' backgrounds in the upward

and downward-looking detectors. The method also requires high-altitude calibration flights to calibrate for aircraft and cosmic background. Analysis of the multichannel spectra indicated that the lower altitude lines (1000m and 2000m) were not radon-free. We found this suprising considering that the lines were flown 10 km offshore and the predominant winds had been from the west-southwest for several days. Perhaps better high-altitude data could be obtained off the southern tip of Tasmania. We have not, as yet, been able to test the method using real data, but this will be done as soon as the first of the 1988 field season data become available for processing.

The GSC method requires no cosmic window and the calibration is less complex. Only a single upward-looking uranium window is used to calculate the uranium window background. The total-count and potassium window backgrounds are then easily calculated from the uranium window background since they are found to be linearly related (Grasty, 1975). This is because variations in all three windows backgrounds are almost entirely related to variations in the concentrations of airborne radon (Grasty & others, 1988)

Of course, the GeoMetrics method could also be used with a single upward uranium window. This would be preferred if it can be established that the uranium background is more accurately determined than the total-count and potassium backgrounds using their method. Having calibrated the BMR system for both techniques, we could also improve on the GSC method by using the continuously monitored 'aircraft+cosmic' background (GeoMetrics method) for T_b. Initial tests using the GSC method have been very encouraging and indicate a vast improvement in background estimation compared with the use of 1000 metre backgrounds. However, any comparison with the GeoMetrics method must await the 1988 field season data.

5. REFERENCES

AVIV, R. and VULCAN, U., 1983 - Airborne gamma-ray survey over Israel: the methodology of the calibration of the airborne system. Israel Atomic Energy Commission, Report No. Z.D. 58/82.

FRITZSCHE, A.E., 1982 - The National Weather Service gamma snow system - physics calibration. Report by Geo-Metrics to National Oceanic & Atmospheric Administration/National Weather Service, by contract with the United States Department of Energy.

GEO-METRICS, 1979 - Aerial gamma ray and magnetic survey, Powder River R+D Project: Final report prepared for the Department of Energy, Grand Junction Office, Grand Junction, Colorado.

GRASTY, R.L., 1975 - Uranium measurements by airborne gamma-ray spectrometry. Geophysics, 40, 503-519.

GRASTY, R.L., 1979 - Gamma-ray spectrometric methods in uranium exploration - theory and operational procedures; in Geophysics and Geochemistry in the Search for Metallic Ores; ed. P.J. Hood, Geological Survey of Canada, Economic Geology Report 31, 147-161.

GRASTY, R.L., WILKES, P.G., and KOOYMAN, R., 1988 - Background measurements in gamma-ray surveys. Geological Survey of Canada Paper 88-11.

MINTY, B.R.S., 1988 - A review of airborne gamma-ray spectrometric data-processing techniques. Bureau of Mineral Resources, Australia, Report 255.

Table 1: Normalised 4-channel cosmic spectrum estimates

Detector	Normalised channel countrates				
	TC	K	U	Th	Cosmic
Single	2.7285	0.1704	0.1607	0.1478	1
Twin	2.7652	0.1678	0.1632	0.1476	1

Table 2: 4-channel aircraft spectrum estimates

Detector	Channel countrates			
	TC	K	U	Th
Single	97.366	17.107	5.515	1.921
Twin	172.940	32.654	8.918	4.271

Table 3: Relative sensitivity of the upward (y) and downward (x) detectors for cosmic and aircraft radiation: linear regression coefficients (y=bx).

Channel	b - single detector	b - twin detector
TC	.2663	.3047
K	.2424	.2804
U	.2871	.3185
Th	.3439	.3415

Table 4: Altitude dependance of the l-sensitivity coefficient: linear regression coefficients (y=a+bx).

Channel	Single detector		Twin detectors	
	a	b	a	b
TC	.1610	-.000107	.1724	-.000121
K	.1675	-.000187	.1709	-.000172
U	.1879	-.000184	.2146	-.000272
Th	.1604	-.000049	.1914	-.000175

Table 5: Altitude dependance of the m-sensitivity coefficient: linear regression coefficients (y=a+bx).

Channel	Single detector		Twin detectors	
	a	b	a	b
TC	.3476	-.000179	.3201	-.000080
K	.2919	-.000081	.3325	-.000149
U	.3167	-.000157	.3084	-.000084
Th	.2363	-.000015	.3824	-.0000084

Table 6: Typical background - component parts

Component	Channel countrates			
	TC	K	U	Th
Total	313.2	31.1	22.1	4.6
Cosmic	33.9	2.1	2.0	2.0
Aircraft	97.3	17.1	5.5	1.9
Radon	182.0	11.9	14.6	0.7

Table 7: Summary of data used to calculate the constants a_1 and a_2 in the method of the Geological Survey of Canada.

PROJECT	LINE	DATA FID LIMITS		BGD FID LIMITS		TH/U
		START	END	START	END	
33	150016	3100	end	start	3080	1.00
33	150026	start	3830	3850	end	1.07
33	150036	4510	end	start	4480	1.20
520	2878	14320	14480	14580	14780	1.29
520	2888	15960	16140	15600	15860	1.34
520	2898	16370	16530	16650	16850	1.28
520	2950	4180	4380	4480	4680	1.29
520	2960	5260	5440	5000	5160	1.26
520	2970	12830	13060	13170	13370	1.25
520	3577	18120	18320	18420	18620	1.25
520	3587	14590	14850	14290	14490	1.28
520	3598	13580	13780	13880	14080	1.31
509	3767	9156	9195	9082	9142	1.46
509	3777	11750	11835	11844	11909	1.44
509	3787	13336	13413	13255	13327	1.74
509	3757	7272	7285	7292	7365	2.67
509	3767	9566	9581	9481	9560	1.67
509	3777	11381	11428	11433	11539	2.45
509	3277	19000	19284	18638	18881	2.37
509	3287	4684	4858	4450	4605	2.24
509	3297	5358	5495	5596	5774	1.97

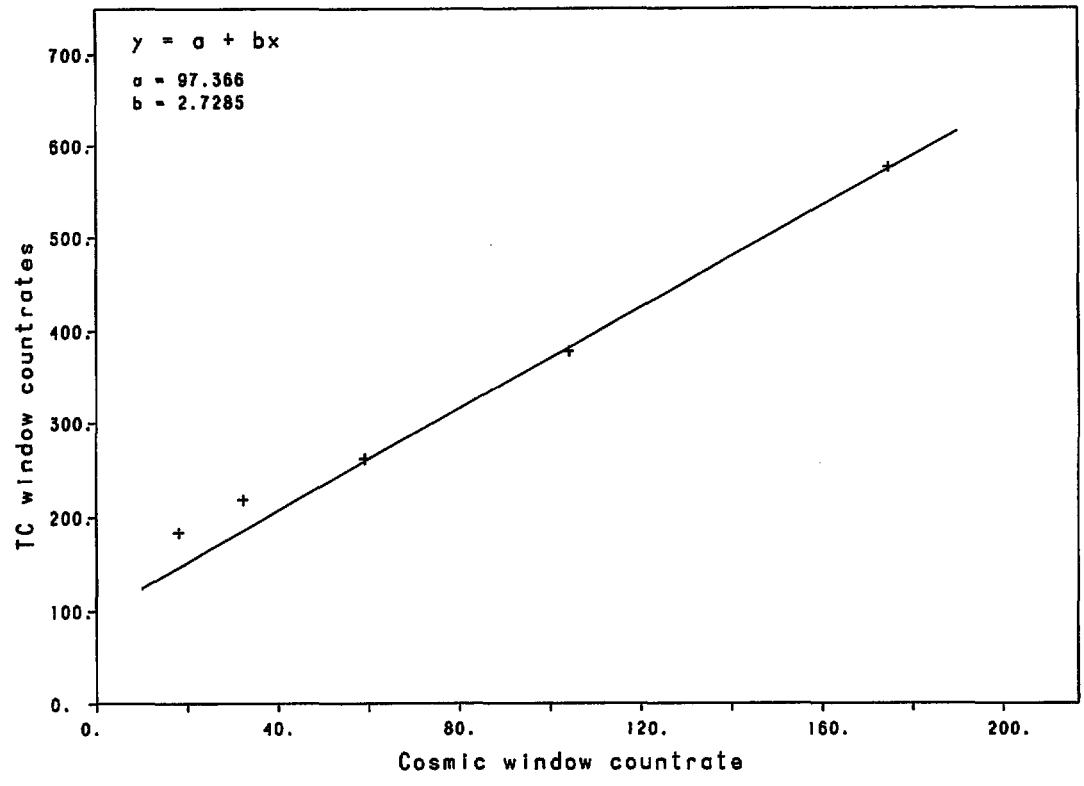

Fig. 1. The relationship between the cosmic window countrate and the TC window background (single detector).

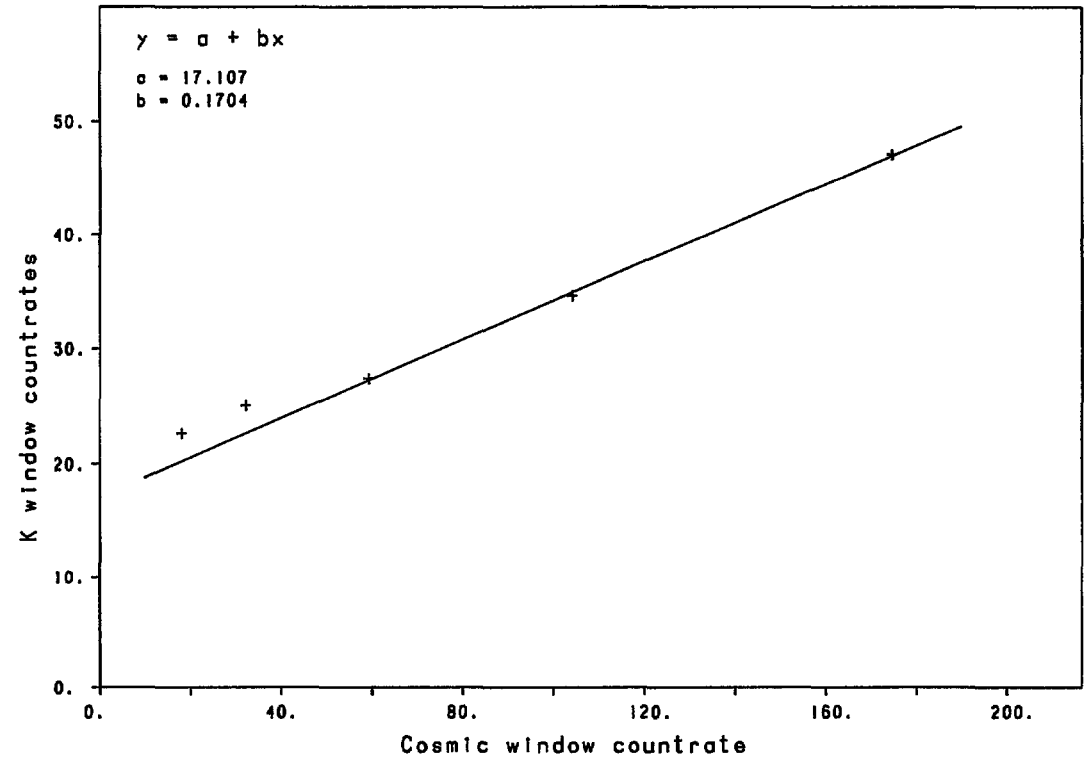

Fig. 2. The relationship between the cosmic window countrate and the K window background (single detector).

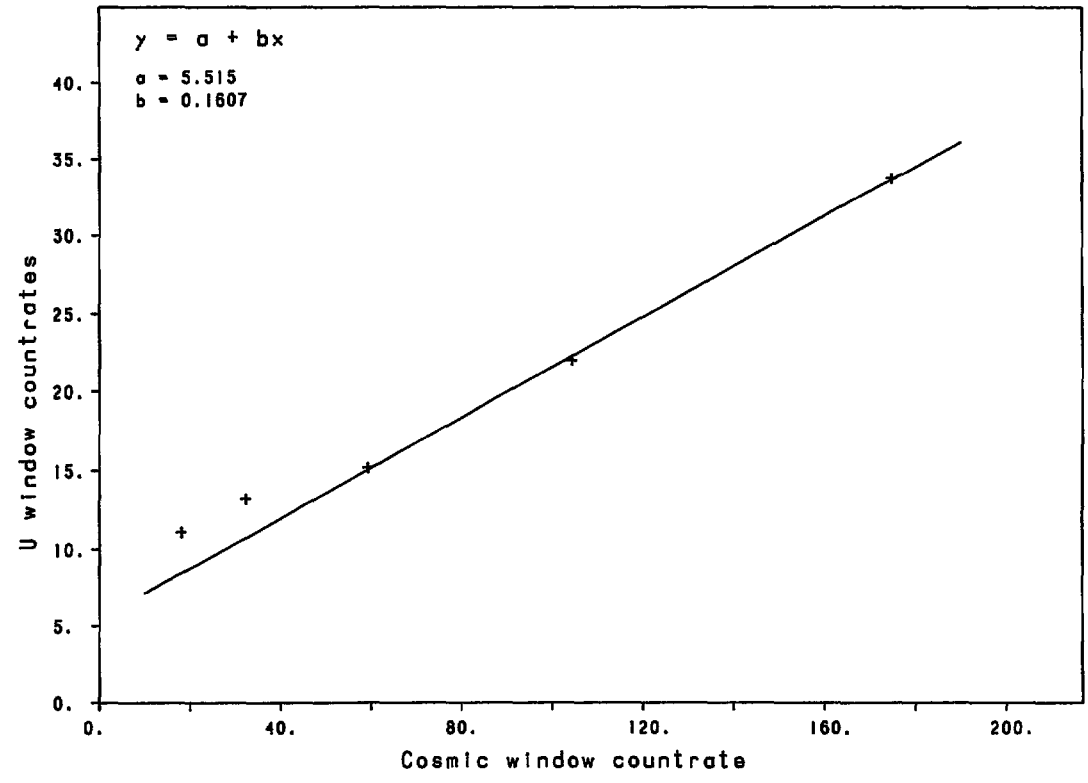

Fig. 3. The relationship between the cosmic window countrate and the U window background (single detector).

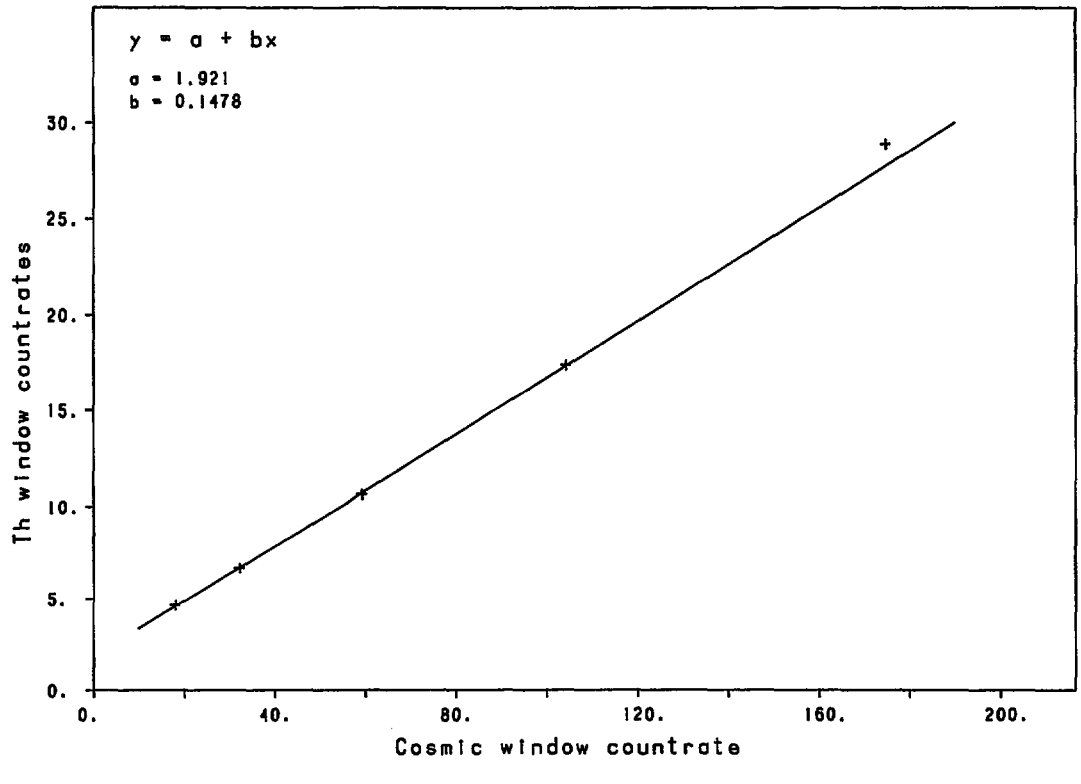

Fig. 4. The relationship between the cosmic window countrate and the Th window background (single detector).

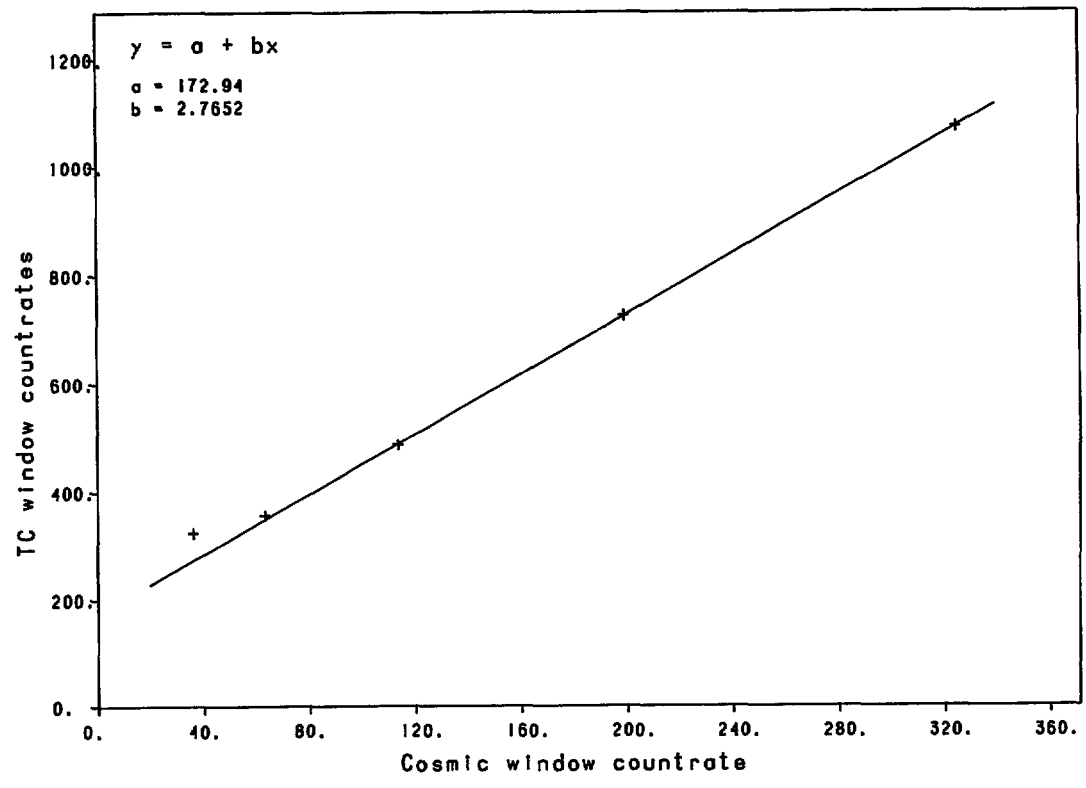

Fig. 5. The relationship between the cosmic window countrate and the TC window background (twin detectors).

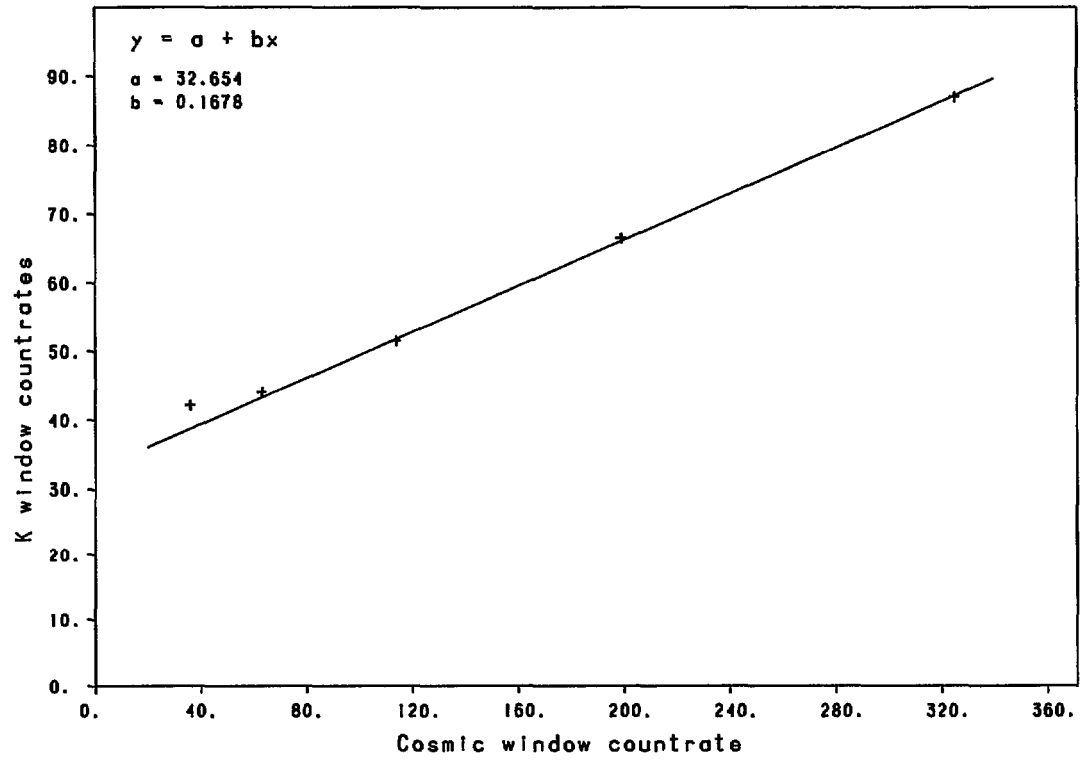

Fig. 6. The relationship between the cosmic window countrate and the K window background (twin detectors).

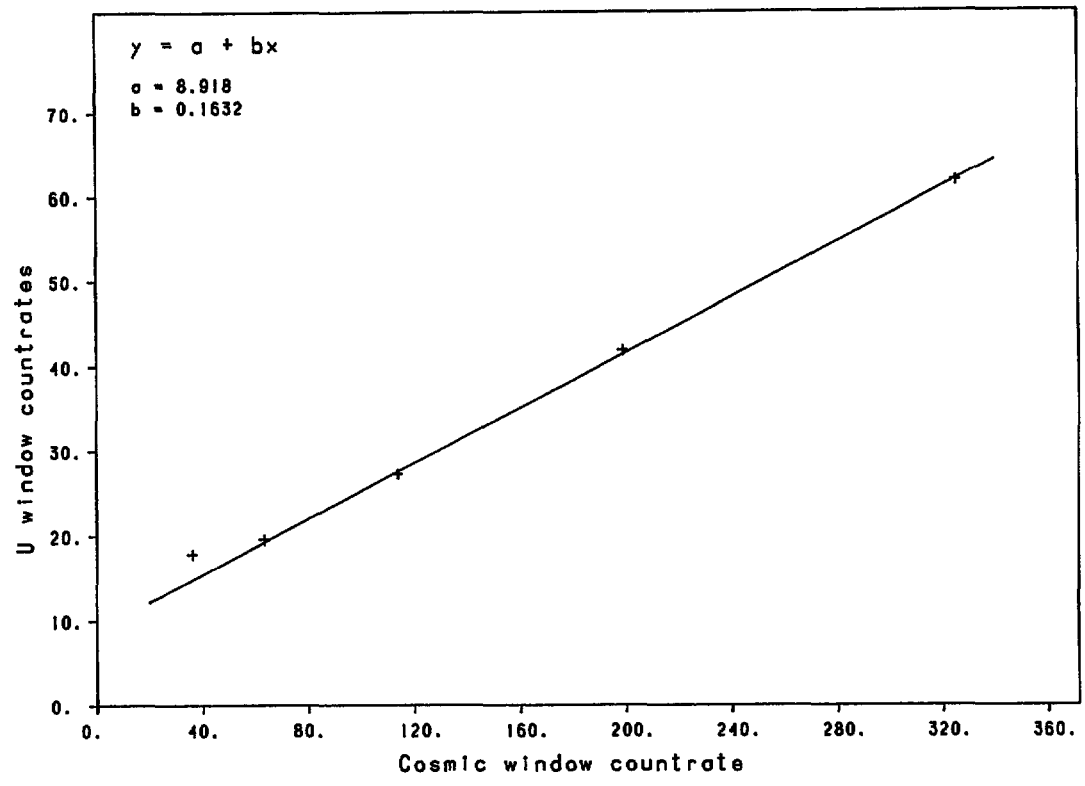

Fig. 7. The relationship between the cosmic window countrate and the U window background (twin detectors).

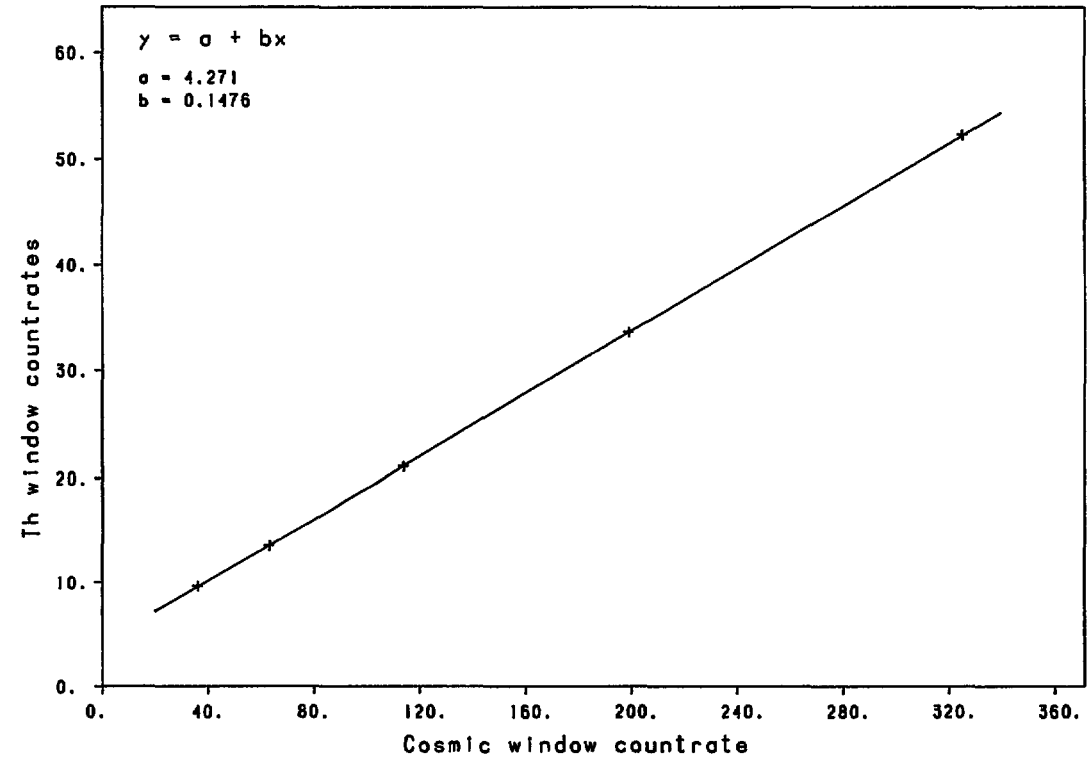

Fig. 8. The relationship between the cosmic window countrate and the Th window background (twin detectors).

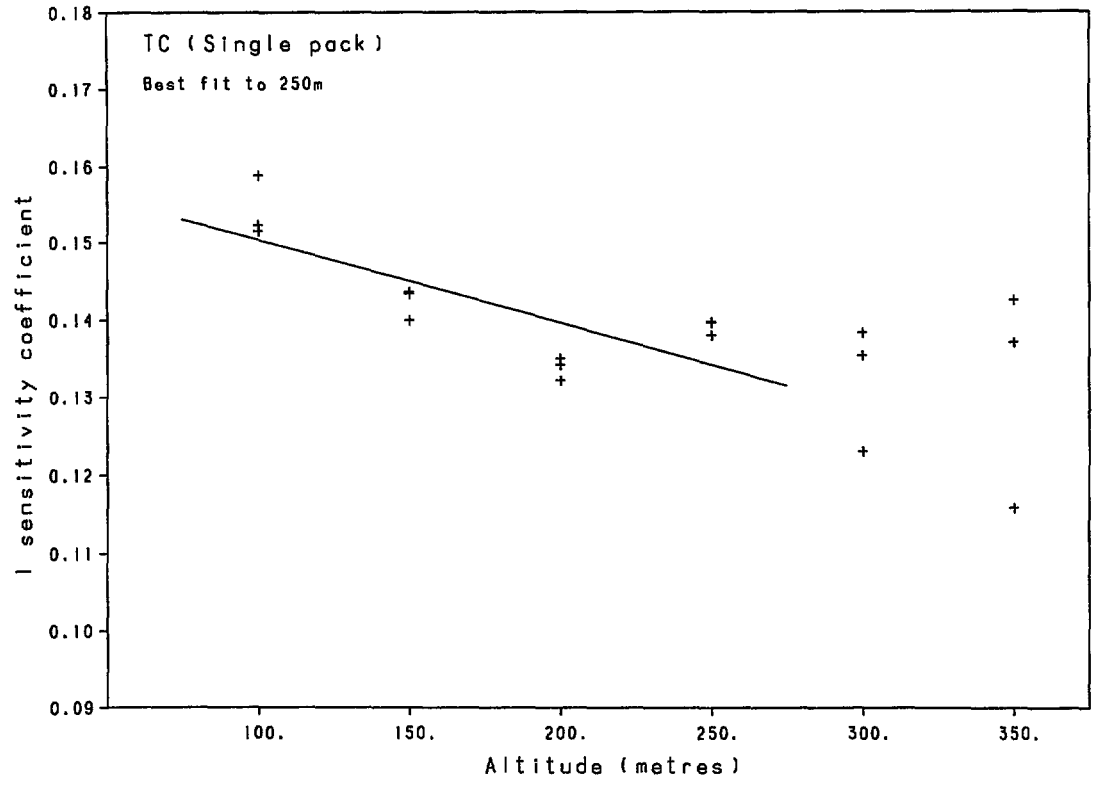

Fig. 9. The relative sensitivity of the upward to the downward-looking detector for terrestrial gamma radiation: Single detector, Total Count window.

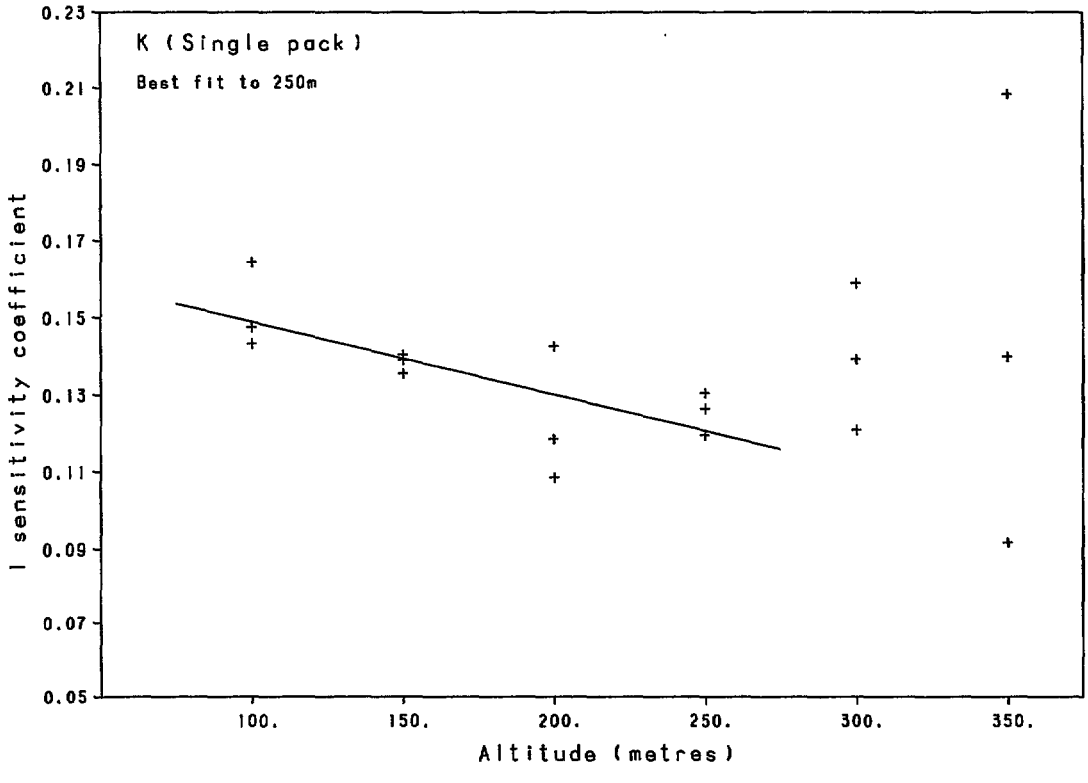

Fig. 10. The relative sensitivity of the upward to the downward-looking detector for terrestrial gamma radiation: Single detector, Potassium window.

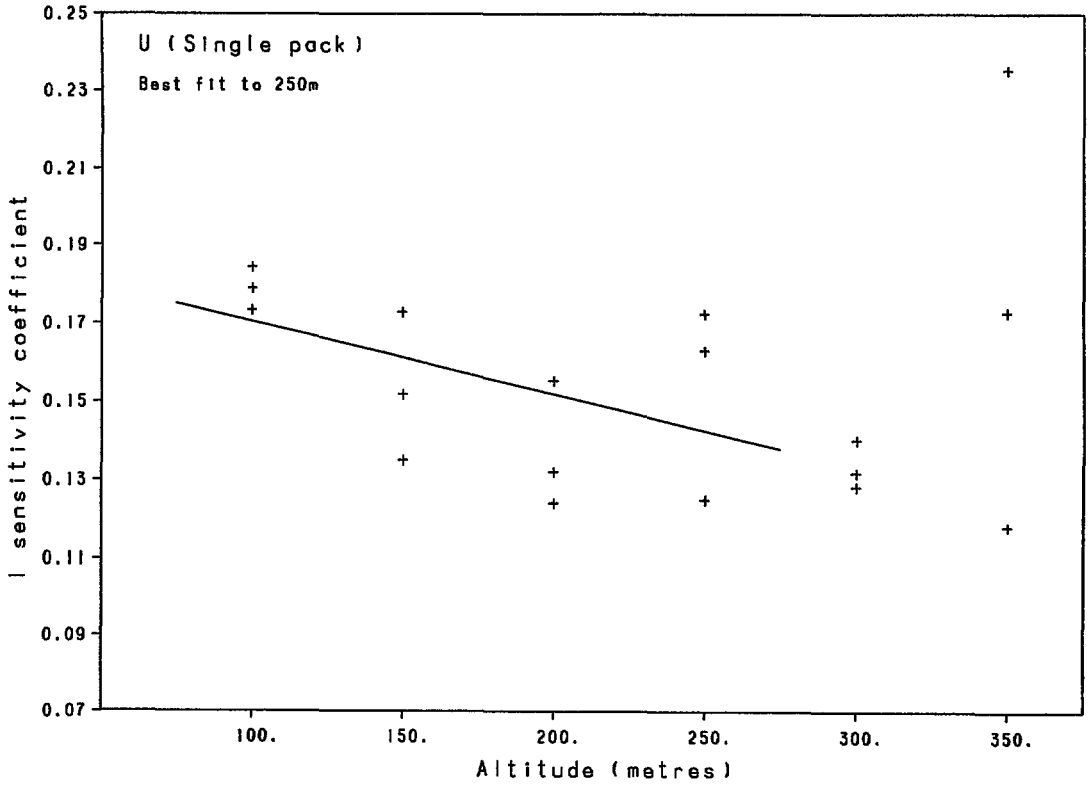

Fig. 11. The relative sensitivity of the upward to the downward-looking detector for terrestrial gamma radiation: Single detector, Uranium window.

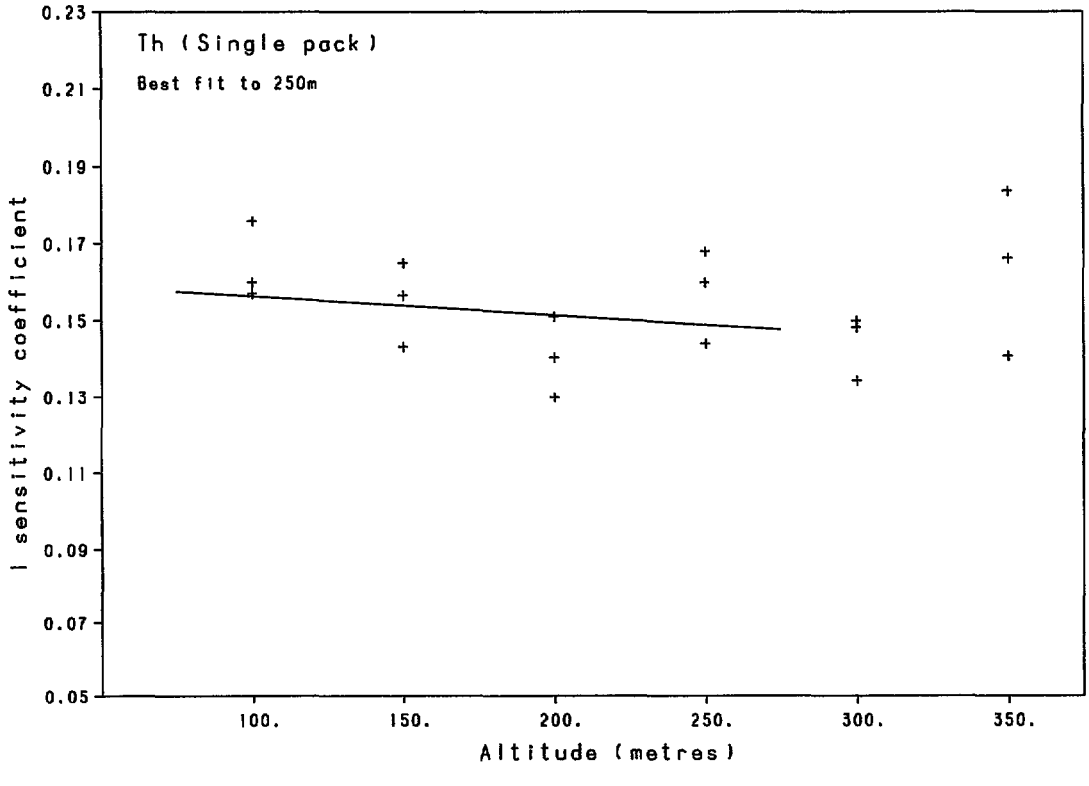

Fig. 12. The relative sensitivity of the upward to the downward-looking detector for terrestrial gamma radiation: Single detector, Thorium window.

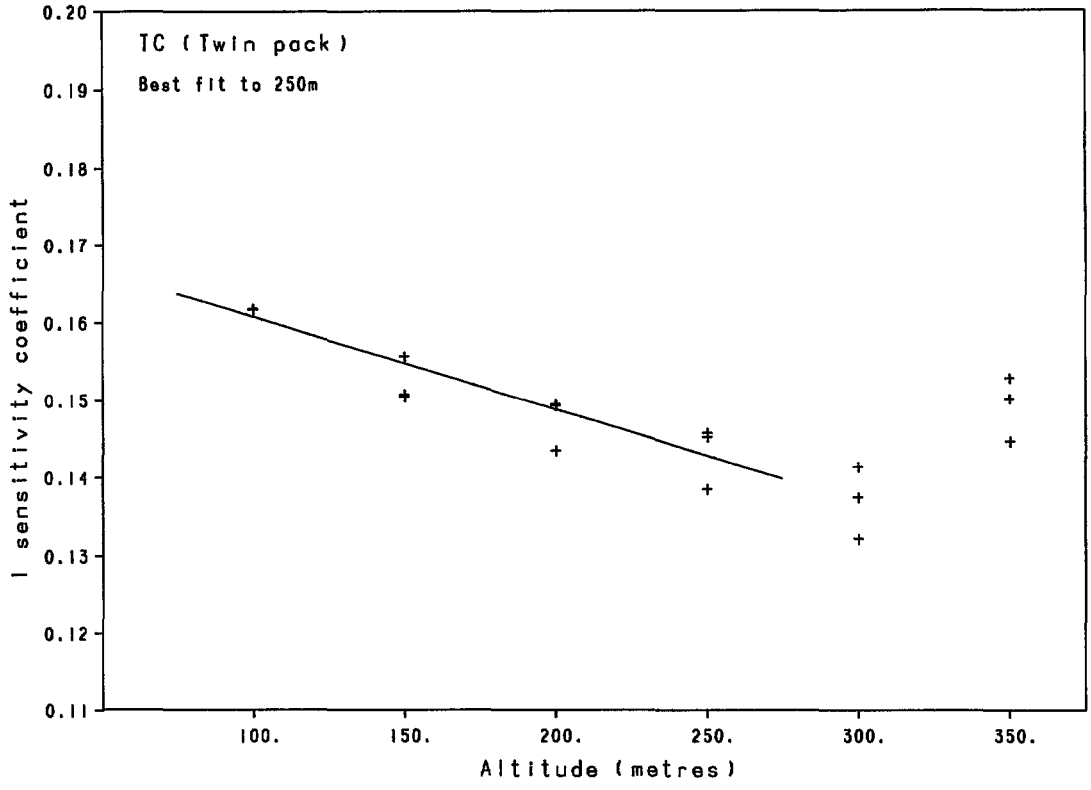

Fig. 13. The relative sensitivity of the upward to the downward-looking detector for terrestrial gamma radiation: Twin detectors, Total Count window.

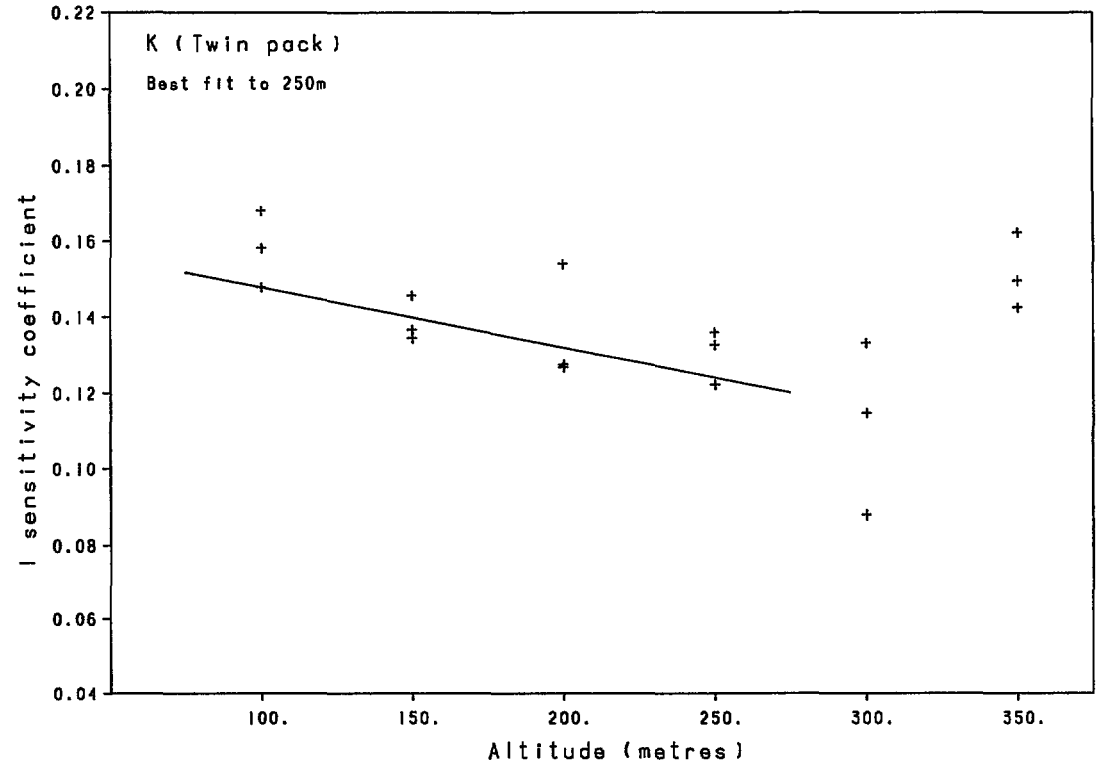

Fig. 14. The relative sensitivity of the upward to the downward-looking detector for terrestrial gamma radiation: Twin detectors, Potassium window.

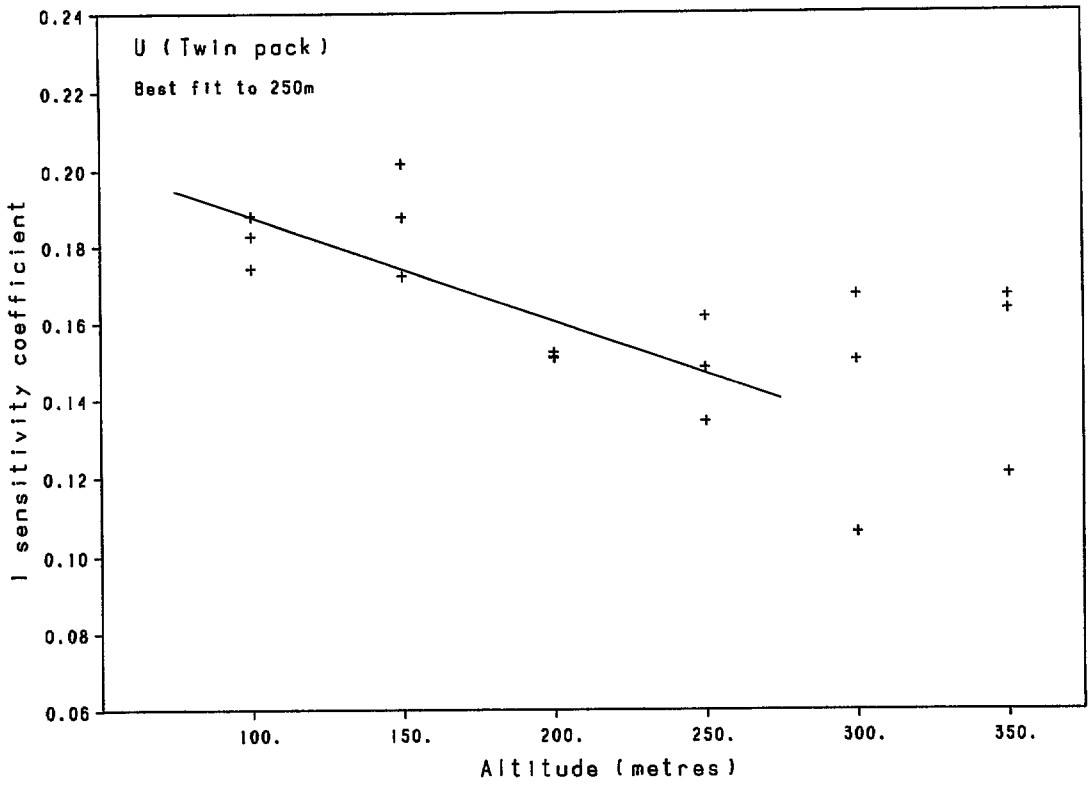

Fig. 15. The relative sensitivity of the upward to the downward-looking detector for terrestrial gamma radiation: Twin detectors, Uranium window.

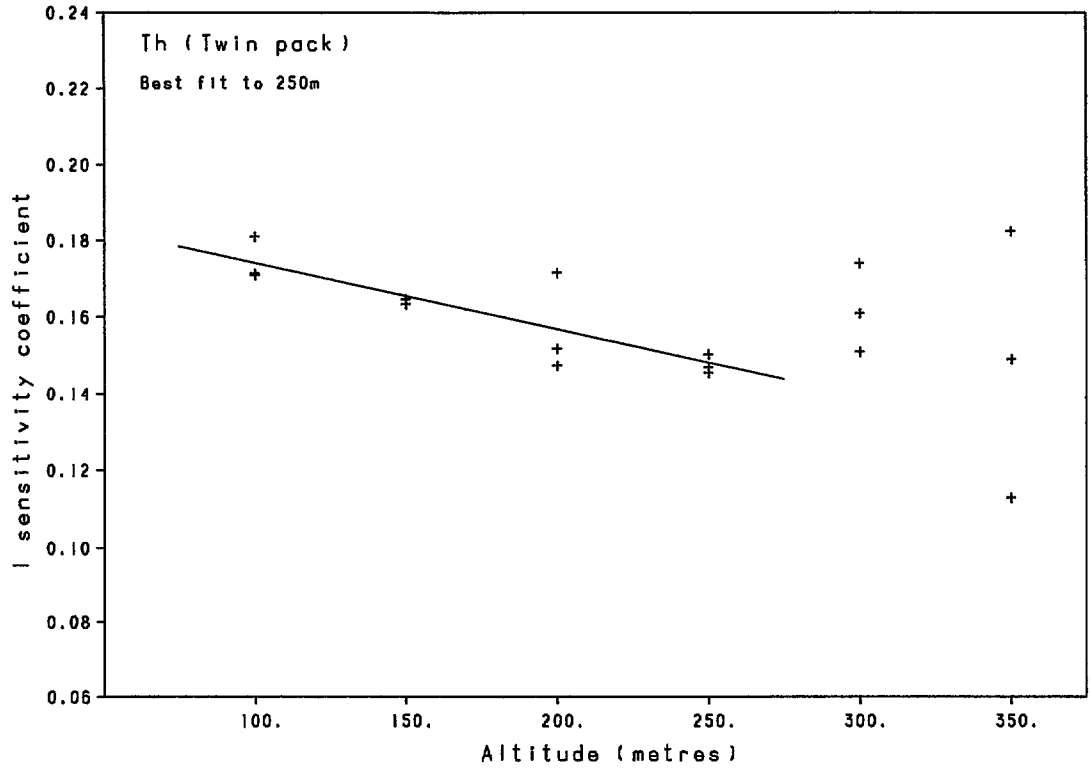

Fig. 16. The relative sensitivity of the upward to the downward-looking detector for terrestrial gamma radiation: Twin detectors, Thorium window.

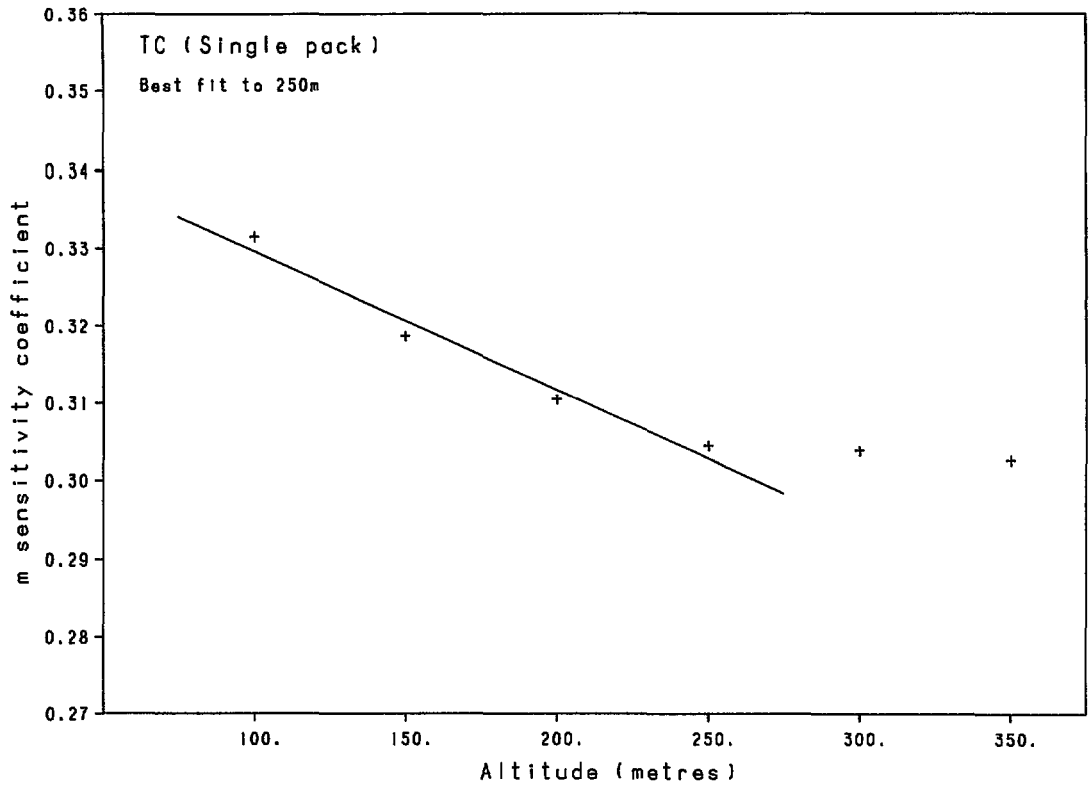

Fig. 17. The relative sensitivity of the upward to the downward-looking detector for atmospheric radiation (radon): Single detector, Total Count window.

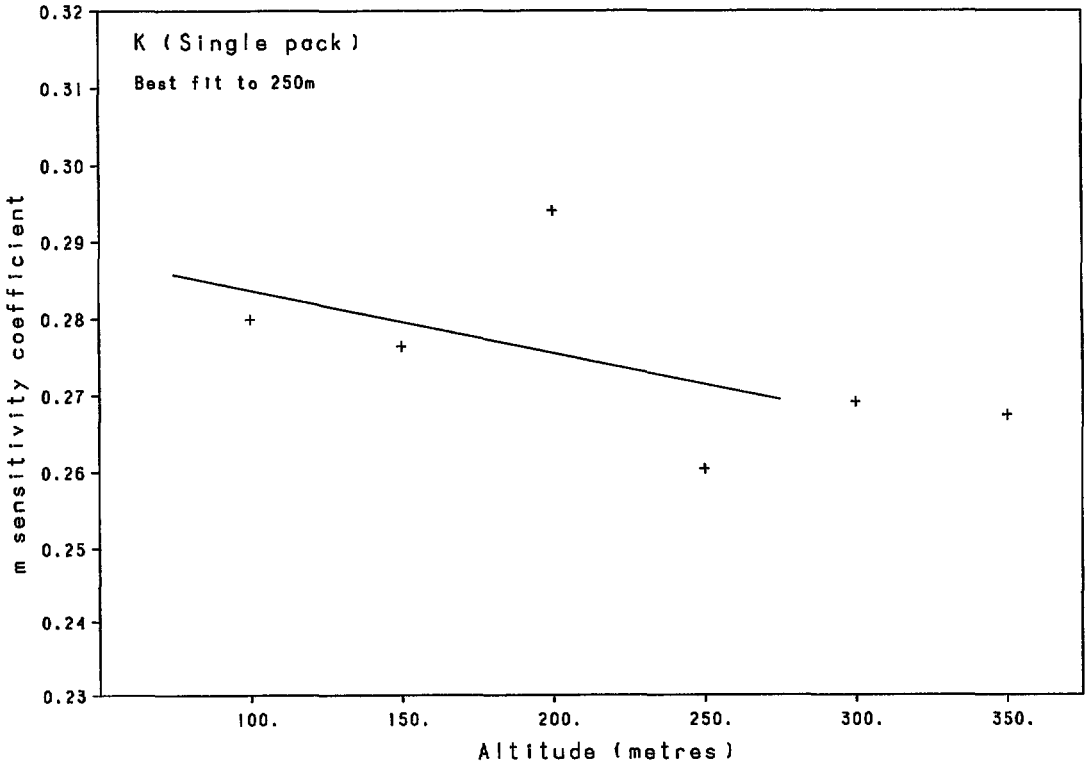

Fig. 18. The relative sensitivity of the upward to the downward-looking detector for atmospheric radiation (radon): Single detector, Potassium window.

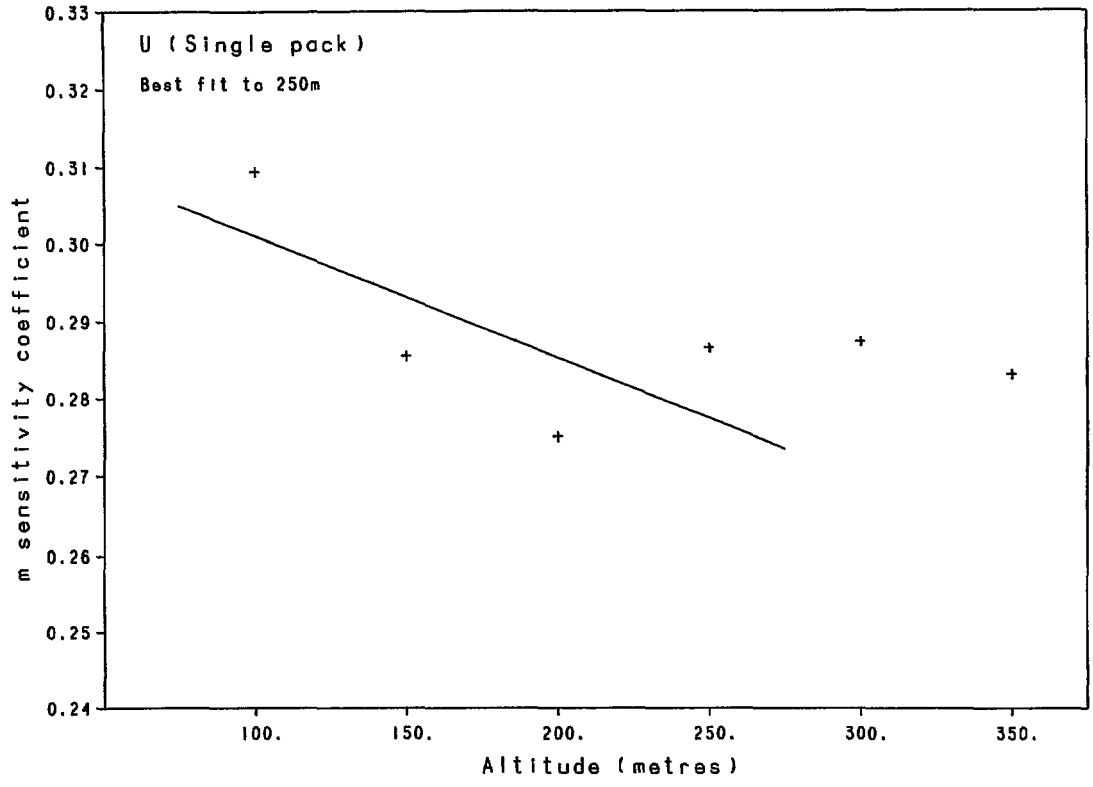

Fig. 19. The relative sensitivity of the upward to the downward-looking detector for atmospheric radiation (radon): Single detector, Uranium window.

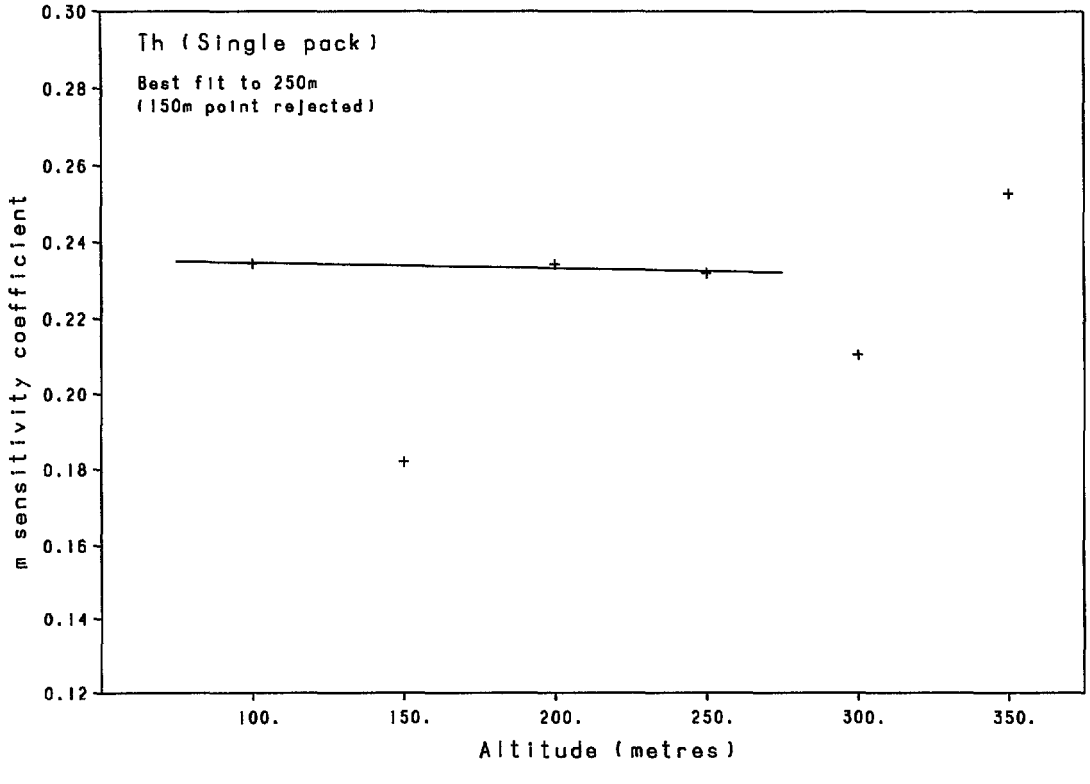

Fig. 20. The relative sensitivity of the upward to the downward-looking detector for atmospheric radiation (radon): Single detector, Thorium window.

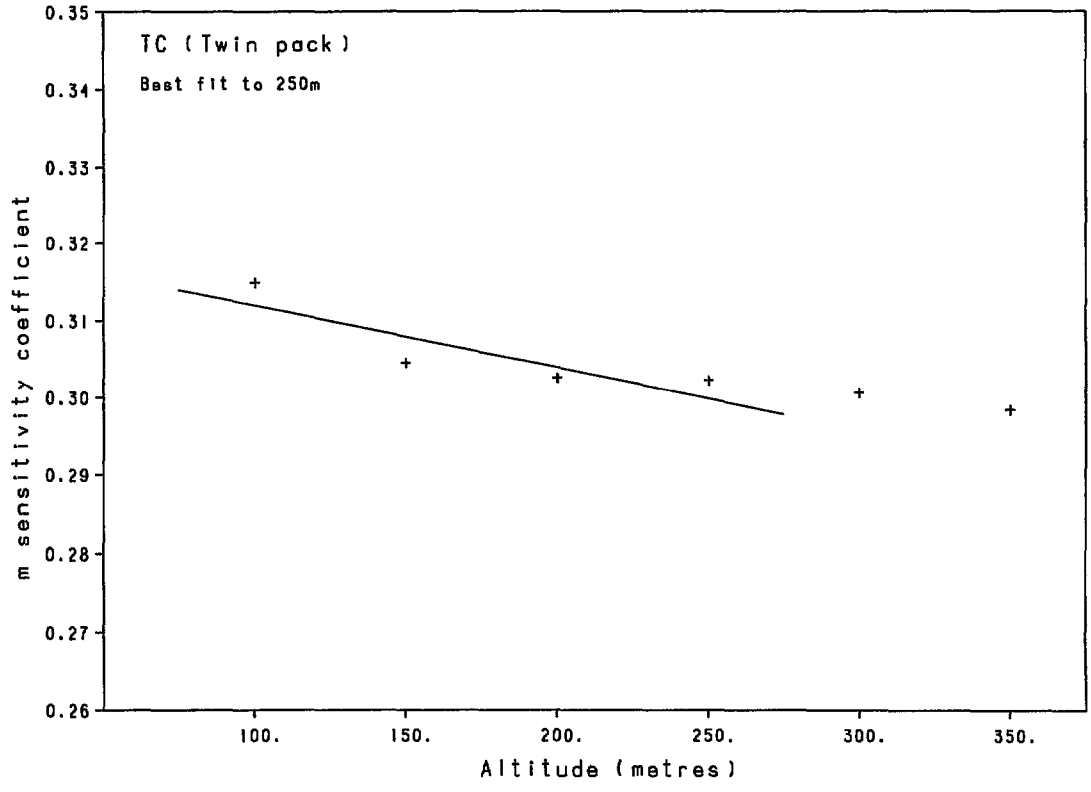

Fig. 21. The relative sensitivity of the upward to the downward-looking detector for atmospheric radiation (radon): Twin detectors, Total Count window.

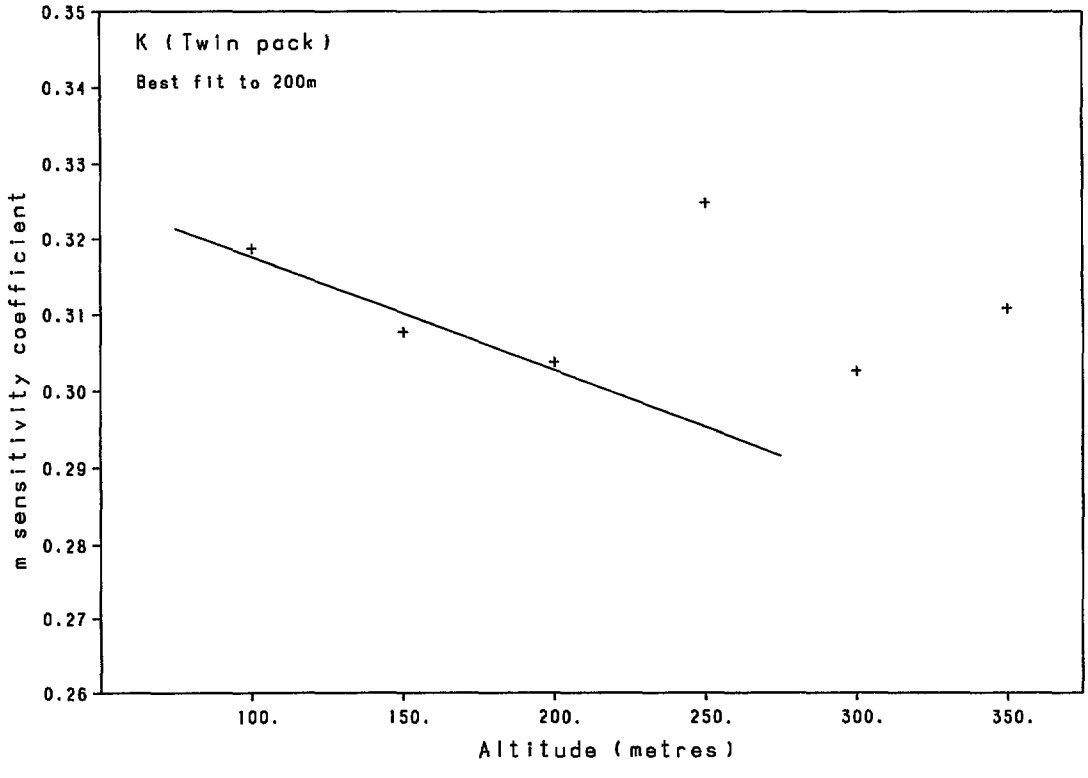

Fig. 22. The relative sensitivity of the upward to the downward-looking detector for atmospheric radiation (radon): Twin detectors, Potassium window.

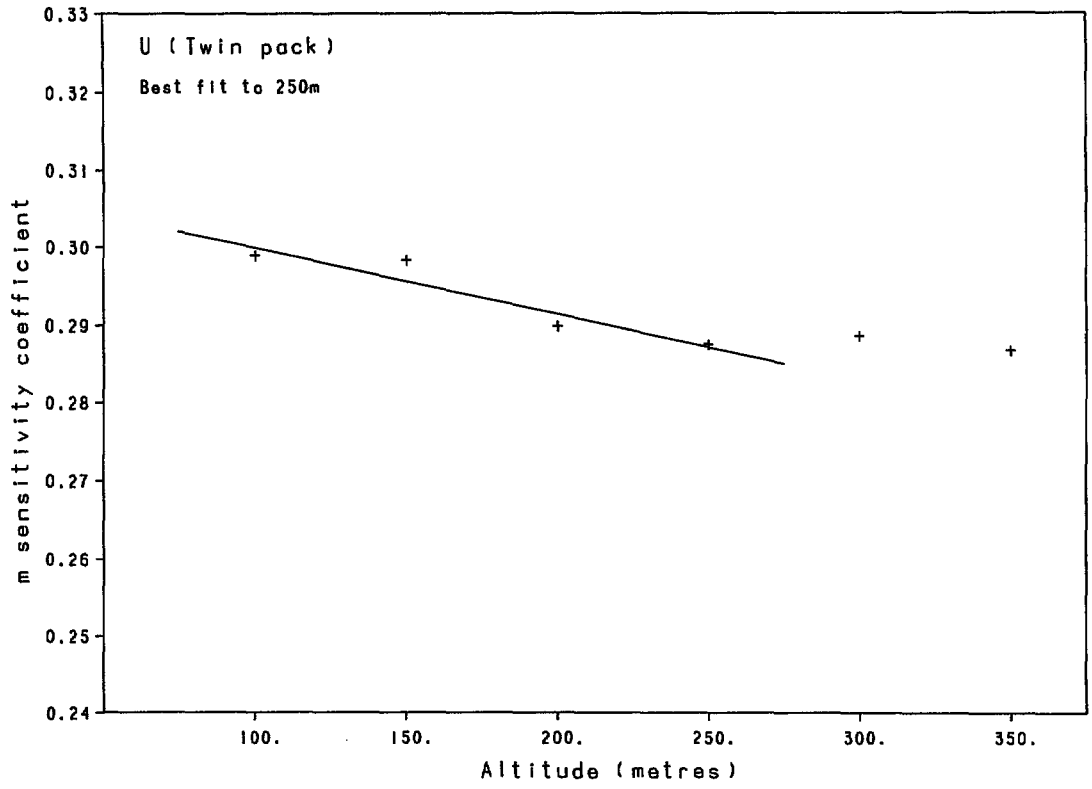

Fig. 23. The relative sensitivity of the upward to the downward-looking detector for atmospheric radiation (radon): Twin detectors, Uranium window.

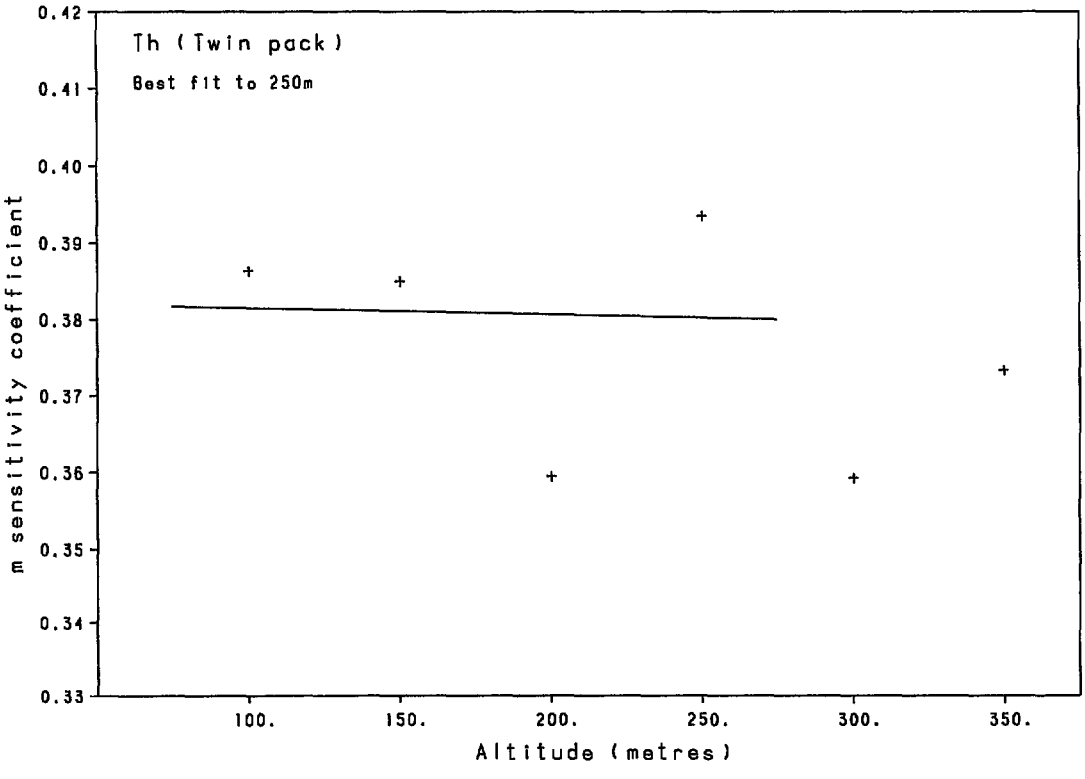

Fig. 24. The relative sensitivity of the upward to the downward-looking detector for atmospheric radiation (radon): Twin detectors, Thorium window.

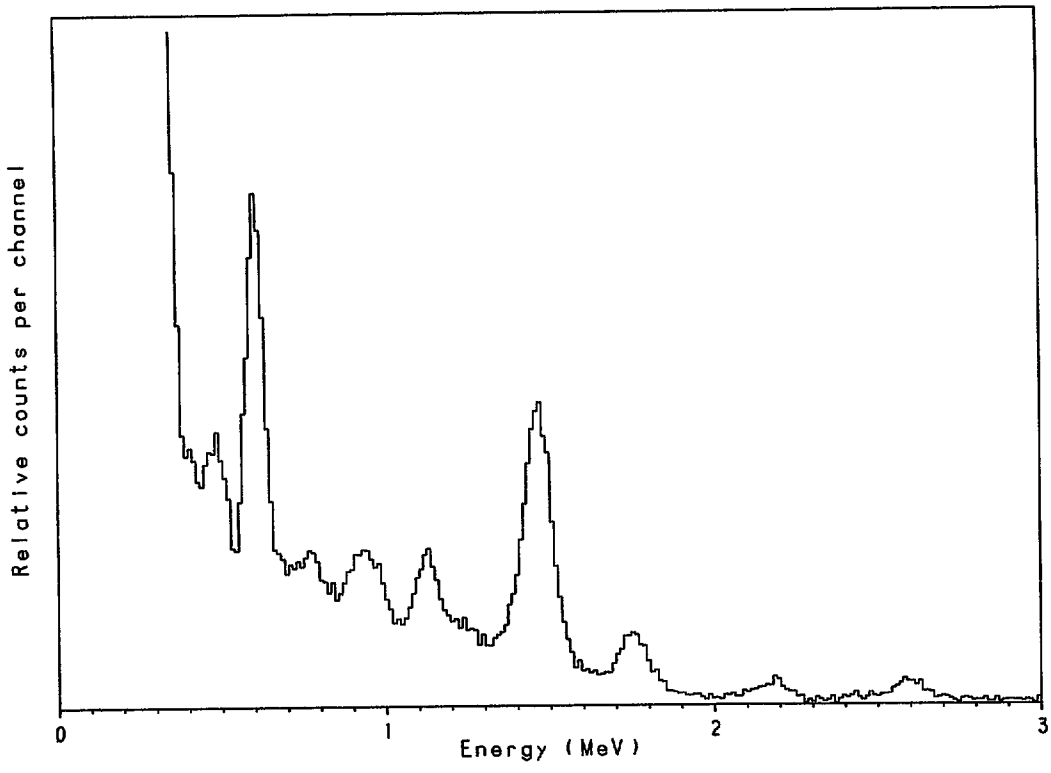

Fig. 25. The aircraft gamma energy spectrum: Twin detectors.

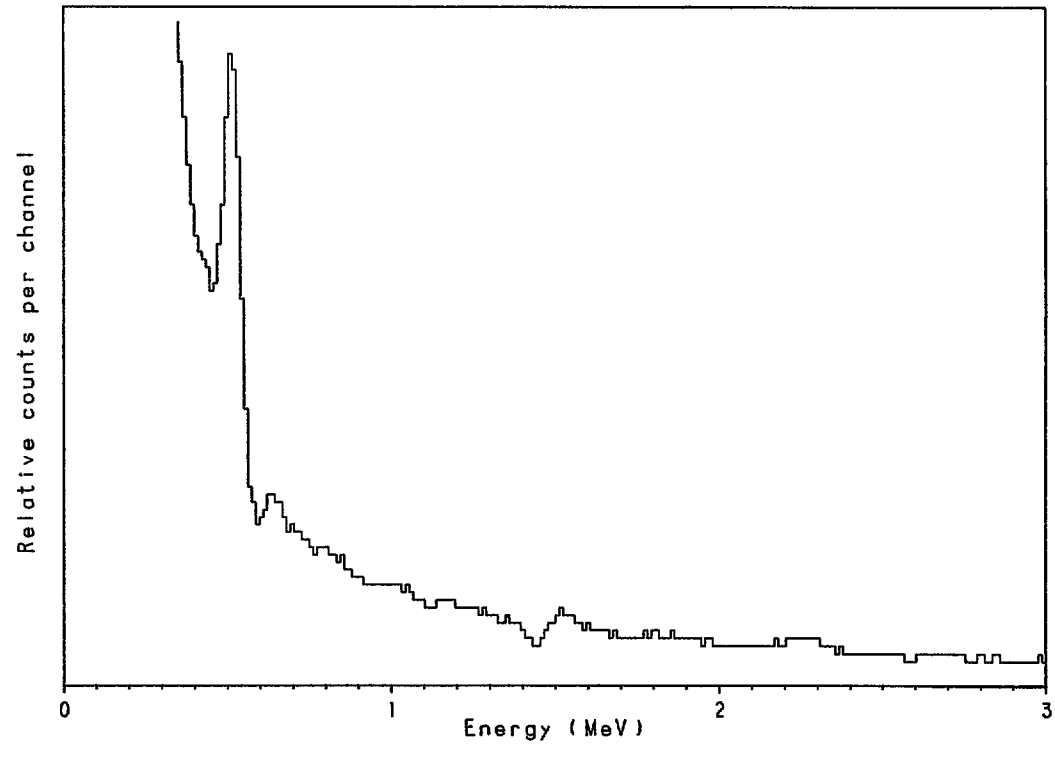

Fig. 26. The cosmic gamma energy spectrum: Twin detectors.

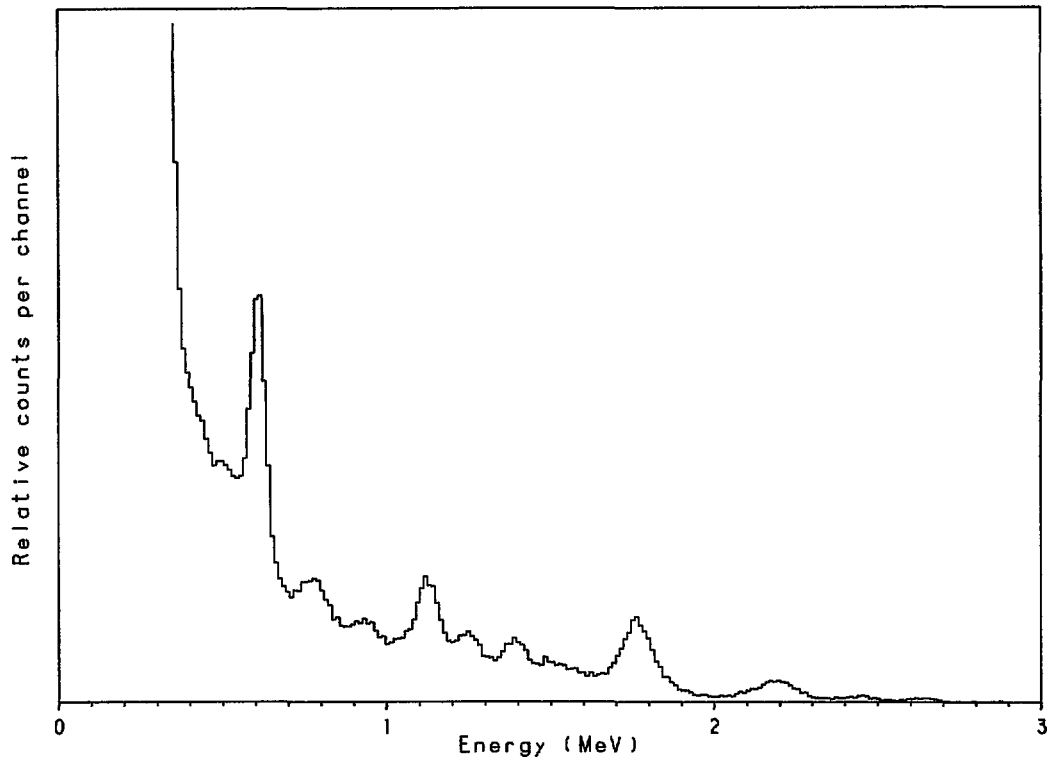

Fig. 27. The radon gamma energy spectrum: Twin detectors.

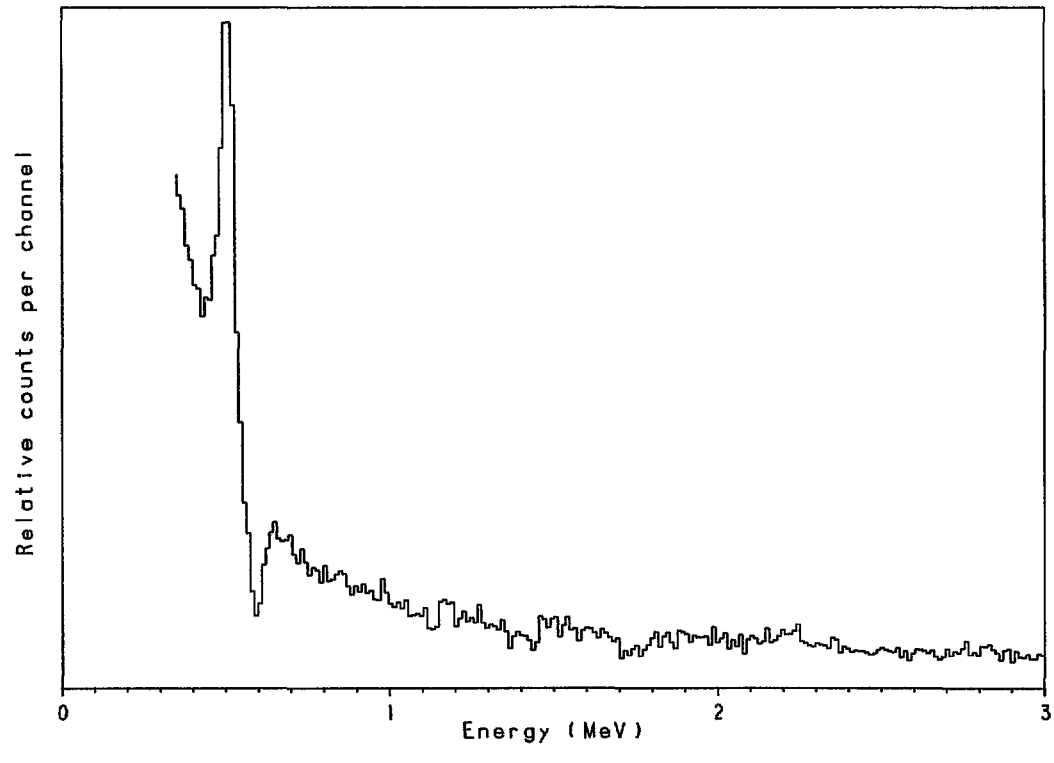

Fig. 28. Radon-corrupted cosmic spectrum estimate.

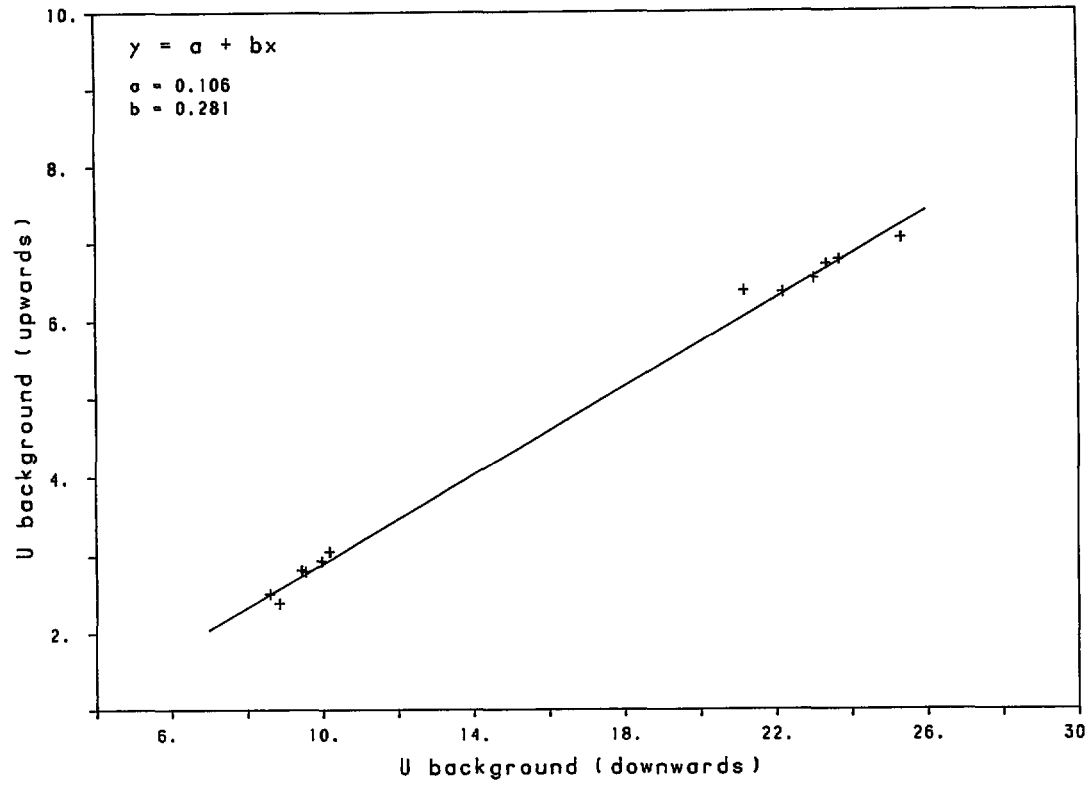

Fig. 29. The relationship between the downward and upward-looking uranium window countrates for background radiation.

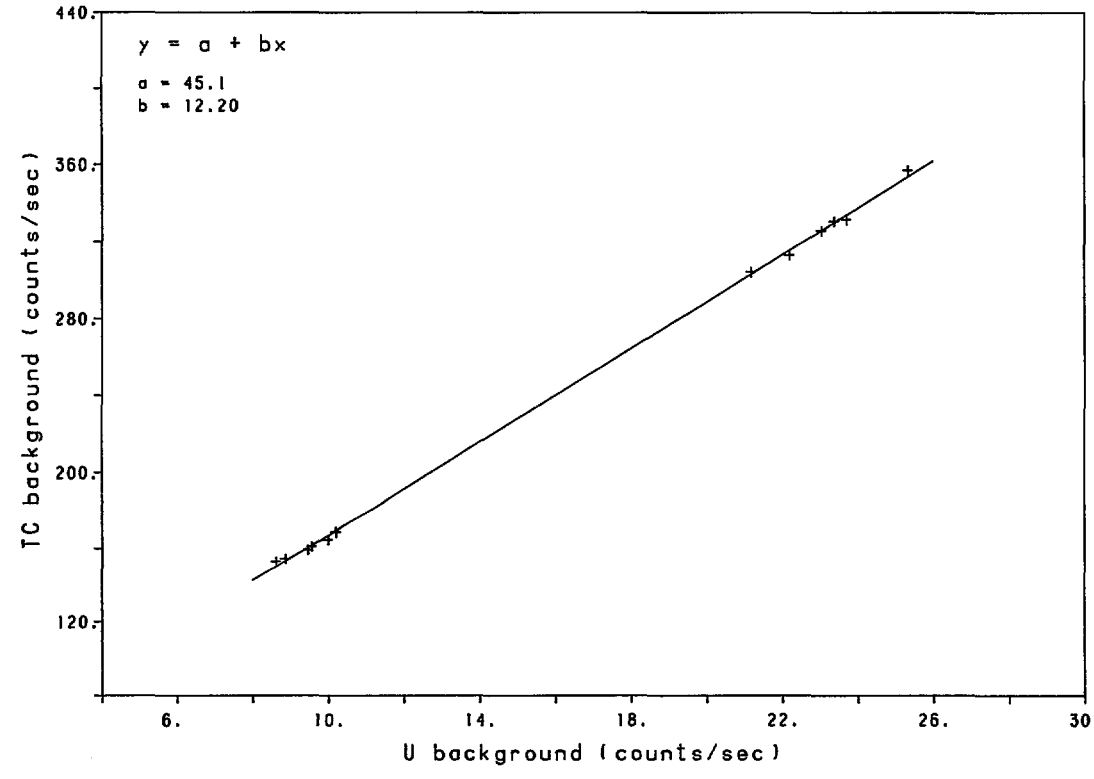

Fig. 30. The relationship between the uranium and total-count window backgrounds.

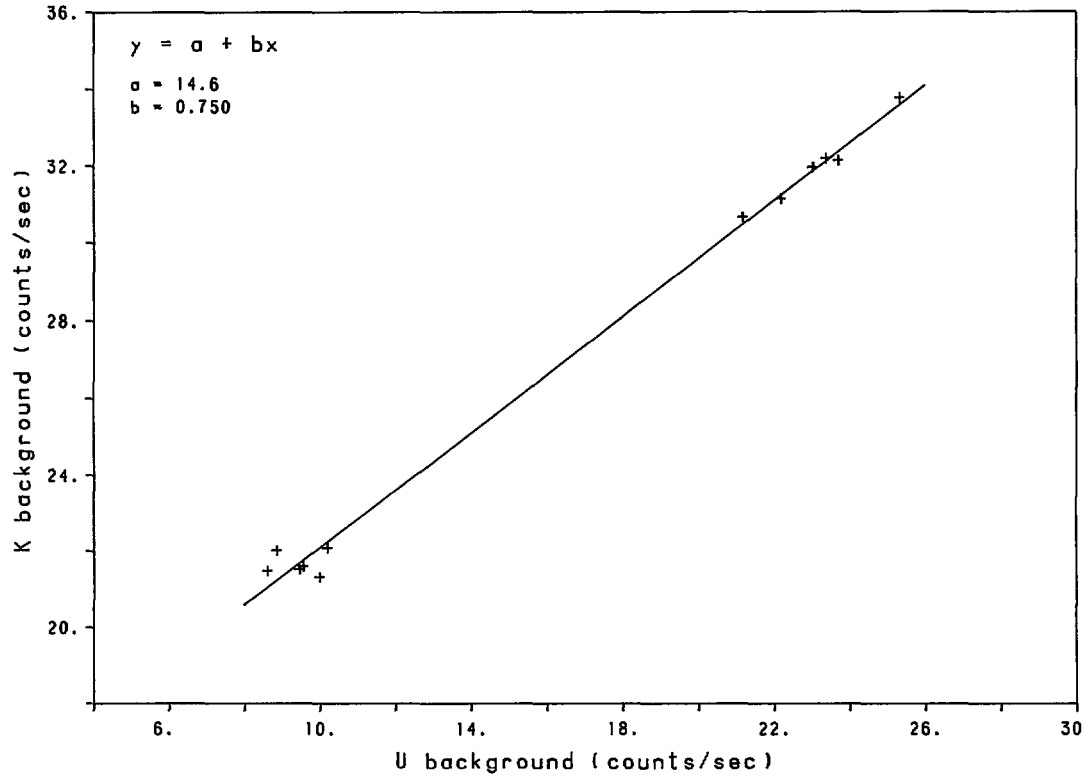

Fig. 31. The relationship between the uranium and potassium window backgrounds.